

Referee 1

Interactive comment on “Aqueous phase oligomerization of methyl vinyl ketone through photooxidation – Part 1: Aging processes of oligomers” by P. Renard et al.

RC C4228: 'Review of Renard et al.', Anonymous Referee #1, 27 Jun 2014

The authors appreciate the many important comments raised by Reviewer 1, which have been considered in the new version of the manuscript. The authors' answers to the questions/comments of Reviewer 1 are presented below.

General:

Question 1

In SOA formation and aging there is competition between oligomerization and oxidation into smaller/volatile species. The discussion of the latter process is missing in the introduction as there is nearly exclusive discussion of oligomerization. So this should be enhanced by mentioning also the generation of volatile species.

Answer

We modified the introduction in order to consider this comment, it now reads:

“ In particular, Renard et al. (2013) showed that $\cdot\text{OH}$ oxidation of MVK in the aqueous phase proceeds via a radical mechanism leading to oligomers which molecular masses increase (up to m/z 1200) with the precursor initial concentration from 2 to 20 mM. At lower precursor initial concentrations (e.g. 0.2 mM of MVK), Renard et al. (2013) observed lower weight molecular compounds (up to m/z 300), and Zhang et al., (2010) observed the formation of small oxidized

compounds (such as acetic, formic, pyruvic acids, methylglyoxal, formaldehyde), thus suggesting a competition between functionalization and oligomerization at these low initial concentrations.”

(...)

“The aim of the present study is to investigate the aging of the oligomers formed through aqueous phase photooxidation of MVK. We determine the SOA chemical composition during the formation and aging of the aqueous phase oligomers and we revisit the corresponding SOA mass yields. A large range of initial precursor concentrations (from 0.2 to 20 mM) is investigated in order to study the competition between functionalization and oligomerization.”

Question 2

In terms of atmospheric relevance, the authors mention wet aerosols and polluted fogs. The concentrations tested here for MVK are in the mM range. Observations in fogs and clouds tend to be in the uM range for the most abundant carbonyls found, so that relevance should be more discussed. The present results appear to suggest (as other studies) that oligomerization does not actually occur in cloud or fog droplets but only in “wet aerosol” where sufficiently high concentrations can be achieved.

In regards to the concentrations used, it would be interesting if the authors would discuss how these compare to the solubility/volatility of MVK and hence the possibility of MVK losses to the gas phase in their experiments and in actual cloud/aerosol situations.

Answer:

In the comparison between our experimental concentrations with atmospheric ones, MVK is considered a proxy for unsaturated water soluble organic compounds (UWSOC). We modified the text accordingly, it now reads:

- In the experimental section:

“Tan et al. (2010) and Renard et al. (2013) have shown the important impact of initial precursor concentrations on oligomer formation. The experiments were thus carried out with various MVK

initial concentrations (Table 1), i.e., 0.2, 0.5, 2, 5 and 20 mM (corresponding to 9.6 to 960 mgC L⁻¹). Considering MVK as a proxy for UWSOC, this concentration range is comprised in the range of the estimated total UWSOC concentrations from fog droplets to wet aerosol (Renard et al., 2013).

The 50 cm³ gas phase head space of the photoreactor was opened to ambient air for a few seconds during each sampling. We verified in control experiments that this procedure induced insignificant losses of MVK from the solution”

- In the section “atmospheric implications”:

“Among the atmospherically relevant alkenoic alcohols, acids, ketones and aldehydes (i.e. UWSOC), although MVK is one of the most abundant species, it is one of the most volatile ($P_{sat} = 10^{-5} - 0.1$ atm, with $P_{sat(MVK)} = 0.1$ atm at 25°C; Asher and Pankow 2006), and one of the least soluble compounds ($K_H = 1 - 10^3$ M atm⁻¹, with $K_{H(MVK)} = 41$ M atm⁻¹ at 25°C; Iraci et al., 1999). The atmospheric impacts of the processes shown here should thus be very limited for MVK alone. However, the oligomerization mechanism undergone by MVK occurs via saturation of the vinyl group (Renard et al., 2013), and the resulting radical monomer is stabilized by the resonance effect with the adjacent carbonyl group thus decreasing the enthalpy of polymerization facilitating the oligomerization in the aqueous phase compared to other molecules. More generally, conjugation of the C=C with substituents such as the benzene ring (styrene and *a*-methylstyrene), and alkene double bond (butadiene and isoprene), the carbonyl linkage (acrylic acid, methyl acrylate, methyl methacrylate), and the nitrile group (acrylonitrile) similarly leads to stabilization of the monomer and decreases enthalpies of polymerization (O'dian 2004). It is thus likely that a large number of atmospherically relevant molecules can follow the same process either in the bulk or at the wet aerosol interface (Kameel et al., 2013; Kameel et al., 2014). In this context, our results suggest that this class of compounds can impact the aerosol composition, and contribute to aqSOA formation upon water evaporation. The corresponding aqSOA mass yields seem to depend on the spectral irradiance of the light used to initiate the photochemistry, but further studies are needed to confirm this point. Finally, the aging of the oligomers formed could be an explanation (at least in part) for the presence the diacids (such as oxalic, malonic and succinic acids) observed in the ambient aerosol (Legrand et

al., 2007; Kawamura et al., 2010). In Part 2 of this study, the atmospheric relevance of these processes is explored by means of multiphase box model studies.”

Question 3a

The manuscript should be able to stand-alone and can be. So please no reference to Renard et al in the abstract (references in abstracts are not common).

Answer:

The abstract was modified according to the reviewer’s comment as well as those of other reviewers, it now reads:

“It has recently been established that unsaturated water soluble organic compounds (UWSOC) might efficiently form oligomers in polluted fogs and wet aerosol particles, even for weakly soluble ones like methyl vinyl ketone (MVK). The atmospheric relevance of these processes is explored by means of multiphase process model studies (in a companion paper). In the present study, we investigate the aging of these aqueous phase MVK-oligomers formed via OH-oxidation, as well as their ability to form secondary organic aerosol (SOA) upon water evaporation. The comparison between aqueous phase composition and aerosol composition after nebulization of the corresponding solutions shows similar trends for oligomer formation and aging. The measurements reveal that oligomer aging leads to the formation of organic diacids. Quantification of the SOA mass formed after nebulization is performed, and the obtained SOA mass yields seem to depend on the spectral irradiance of the light used to initiate the photochemistry. Investigating a large range of initial MVK concentrations (0.2 – 20 mM), the results show that its \cdot OH-oxidation undergoes competition between functionalization and oligomerization that is dependent on the precursor concentration. At high initial MVK concentrations (≥ 2 mM), oligomerization prevails over functionalization, while at lower initial concentrations, oligomerization is not the major process, and functionalization dominates, resulting in small carbonyls, dicarbonyls and monoacids. The atmospheric implications of these processes are discussed.”

Question 3b:

Then in your discussion, please present first your results and then discuss them relative to your group's earlier work and not start by saying e.g. 15292L16 "In good agreement with our previous results (Renard et al., 2013), after 5 min of reaction (experiment B),": Please first your results, then comparisons otherwise the text does not stand on its own.

Answer:

The text has been modified according to this comment, it now reads:

"During experiment B (i.e. $[MVK]_0 = 5mM$), after 5 minutes of reaction, no significant formation of high molecular weight compounds (HMWC) was observed (Figure 2b), whereas after 10 minutes of reaction, mass spectra show that oligomer systems were formed on the whole range of the investigated m/z (50-1200), with a regular pattern of 70.042 amu, which corresponds to the exact mass of MVK. At 50 minutes of reaction, the maximum of oligomerization was reached (Figure 2c). At this time, we observed several series of MVK-oligomers, corresponding to several initiator radicals identified by Renard et al. (2013) under the same conditions."

Question 4

The lamp characterization is excessively vague in the experimental section and then in the comparison with Liu. As this seems to matter please provide the actual values you measured as you use a 1000W lamp you get only twice ambient irradiation when many investigators (including Liu et al., 2012) use 300W lamps to get ambient irradiation fluxes. The irradiation and its realism should also be mentioned in the section on atmospheric relevance

Answer:

The different irradiation Xe lamp intensities used: 300 W in Liu et al. (2012), and 1000 W in the present study, have been measured using a spectroradiometer (SR-501, LOT-Oriel). The same spectroradiometer has been used to measure the direct solar irradiance intensity at sea level, for a 48.3° zenith angle and is given as a comparison and these data are now shown in Figure S1.

We modified the text to be more precise on the lamp spectral irradiance:

- In the experimental section:

“The photoreactor set-up used was based on the one described by Renard et al., (2013). It was a 450 cm³ Pyrex thermostated photoreactor, equipped with a 1000 Watt Xenon arc lamp (LOT-Oriel, LSH 601) and a glass filter (ASTM 490 AM 0). The resulting spectral irradiance into the reactor is compared to that of the sun at sea level for a 48.3° zenith angle in Figure S1.”

- in section 3.2.3:

“The different yields obtained here as compared to the study by Liu et al. (2012) may be due to the different irradiation Xe lamp used: 300 W (with a pyrex filter) in Liu et al. (2012), and 1000 W (with a ASTM 490 AM 0 filter) in the present study. The influence of the lamp spectra on SOA mass yields of other systems (gas phase photooxidation of biogenic and anthropogenic precursors) have been previously observed in atmospheric simulation chambers (Bregonzio-Rozier et al., 2014). We verified, using a spectroradiometer (SR-501, LOT-Oriel), that the spectral irradiance of the 300W and the 1000W Xe lamps at $\lambda \geq 400$ nm represent respectively half and twice the solar irradiance intensity at sea level, for a 48.3° zenith angle (Figure S1). Due to the high variability of the irradiance in the atmosphere at $\lambda \geq 400$ nm (as shown by the Tropospheric Ultraviolet and Visible Radiation Model http://cprm.acd.ucar.edu/Models/TUV/Interactive_TUV/), both lamps can be seen as representative of the natural irradiance in this wavelength range. However at 300 nm, the spectral irradiance of the 1000W Xe lamp is 7 and 9 times higher than that of the direct solar irradiance (for a 48.3° zenith angle) and the 300W Xe lamp respectively (Figure S1). This part of the spectrum is essential for photochemistry, and may induce different photochemical processes: we verified that we observed the same series of oligomers as in Liu et al. (2012), but with different relative intensities. The different spectral irradiance of the lights used at 300 nm

may be the reason for the different yields obtained, but it needs to be confirmed by a thorough study of the influence of the spectral irradiance (in the UV) on the oligomer mass yields.”

Details:

Question 5:

Abstract and text: Not everybody is familiar with AMS language, OOA etc: : : would need to be explained at first use, not only later on in the discussion. You use the terms in the abstract and you don't define but you define UWSOC but do not use the abbreviation in the abstract.

Answer:

This remark was taken into account: see the new abstract reported in our answer to question 3.

Question 6:

The experimental section looks a little sloppy. Please homogenize language and explanations. In some instances instruments are mentioned without the manufacturer, while others have manufacturer and location given in parentheses. Idem for the chemicals used.

Answer:

Done

Question 7:

15289L13 shouldn't deprotonated molecules be [M]- or [M(-H)]+ or something different as is looks too similar to [M-H]+.

Answer:

We used the IUPAC (2013) recommendations (Murray et al., 2013):

[M+H]⁺ for protonated molecules

[M - H]⁻ for deprotonated molecules

Question 8:

Some text is bizarre in regard to how numbers/ranges are presented: “A yield of 595% (in mass) was obtained with this method at 90 min of reaction, thus statistically similar from the one obtained by the nebulizing method (750 %) at tmax.” 7 +-50%? I assume it is 50+-7%?

Answer:

Yes, this was a typo that was corrected in the new version of the manuscript

Question 9:

15298L24 again bizarre, please write “50-120%” not 120-50%

Answer:

Done

Question 10:

15295 first paragraph: use the same notation in the explanation of the terms than in the formula and in the next lines C/O not C:O

Answer:

Done

Question11:

15294L9 for the non AMS community it would be good to explain or mention what the correction factors are used for? Please explain its reason of being.

Answer:

The AMS collection efficiencies (CE) were investigated by comparing AMS to SMPS measurements. The AMS collection efficiency represents the efficiency with which particles are transmitted through the aerodynamic lens system and the particle time-of-flight (PToF) chamber, as well as the bouncing effect on the vaporizer surface (Huffman et al., 2005, Docherty et al., 2013; Miyakawa et al., 2013). In addition to these effects, it is possible that our low CE values (compared to chamber studies or ambient aerosols) were also due to the particle size range (50 nm - 150 nm mass distribution), as the lowest part of this size range corresponds to the region where the AMS transmission curve varies greatly (Liu et al., 2007). This effect is confirmed by the fact that our lowest values for CE (0.07) were obtained for the lowest MVK initial concentrations (0.2 – 2 mM) where the smallest particles were formed (50 nm mass distribution).

The text was modified, it now reads:

“Note that the overall collection efficiencies (CE) of the AMS in our experiments varied from 0.07 to 0.21 (related to the SMPS signal). These low CE values (compared to chamber studies or ambient aerosols) can be due to particle bounce at the vaporizer surface before volatilization and to the shape and size-dependent transmission of the aerodynamic lens. As a result, the studied compounds did not volatilize sufficiently fast at standard AMS vaporizer temperatures to be fully detected (Liu et al., 2007; Docherty et al., 2013; Miyakawa et al., 2013). In addition to

these effects, it is possible that our low CE values were also due to the particle size range (50 nm - 150 nm mass distribution), as the lowest part of this size range corresponds to the region where the AMS transmission curve varies greatly (Liu et al., 2007). This effect is confirmed by the fact that our lowest values for CE (0.07) were obtained for the lowest MVK initial concentrations (0.2 – 2 mM) where the smallest particles were formed (50 nm mass distribution).”

Language:

The manuscript could benefit from English editing.

Answer:

Done

Figures:

Figure 1: panels b,c and d do not have the same scale so I see no reason why to have panel b with a scale such that one can hardly see the mass spectrum. Idem panel d. the small peaks would only make sense if all panels had same scale on the y axis Panel c: hard to see the underlying spectrum with the red over it. Why not prepare a figure like figure 4 or stagger the spectra.

Figure 3: the panels and legends are very small and will end up being hard to read

Figure 5: legend of 5a partly covered by fig 5b Figure 5: are the units on y axis right?

Figure 6: show MVK consumed in % or mention in the legend how much MVK was present initially? 5mM?

Answer:

All these modifications were done in the new version of the manuscript

In figure 5 the units on Y axis are right.

References

- Asher, W. E. and Pankow, J. F.: Vapor pressure prediction for alkenoic and aromatic organic compounds by a UNIFAC-based group contribution method, *Atmospheric Environment*, 40(19), 3588–3600, doi:10.1016/j.atmosenv.2005.12.004, 2006.
- Brégonzio-Rozier, L., Siekmann, F., Giorio, C., Pangui, E., Morales, S. B., Temime-Roussel, B., Gratien, A., Michoud, V., Ravier, S., Tapparo, A., Monod, A. and Doussin, J.-F.: Gaseous products and Secondary Organic Aerosol formation during long term oxidation of isoprene and methacrolein, *Atmospheric Chemistry and Physics Discussions*, 14(16), 22507–22545, doi:10.5194/acpd-14-22507-2014, 2014.
- Docherty, K. S., Jaoui, M., Corse, E., Jimenez, J. L., Offenberg, J. H., Lewandowski, M. and Kleindienst, T. E.: Collection Efficiency of the Aerosol Mass Spectrometer for Chamber-Generated Secondary Organic Aerosols, *Aerosol Science and Technology*, 47(3), 294–309, doi:10.1080/02786826.2012.752572, 2013.
- Huffman, J. A., Jayne, J. T., Drewnick, F., Aiken, A. C., Onasch, T., Worsnop, D. R. and Jimenez, J. L.: Design, Modeling, Optimization, and Experimental Tests of a Particle Beam Width Probe for the Aerodyne Aerosol Mass Spectrometer, *Aerosol Science and Technology*, 39(12), 1143–1163, doi:10.1080/02786820500423782, 2005.
- Iraci, L. T., Baker, B. M., Tyndall, G. S. and Orlando, J. J.: Measurements of the Henry's law coefficients of 2-methyl-3-buten-2-ol, methacrolein, and methylvinyl ketone, *Journal of atmospheric chemistry*, 33(3), 321–330, 1999.
- Kameel, F. R., Hoffmann, M. R. and Colussi, A. J.: OH Radical-Initiated Chemistry of Isoprene in Aqueous Media. Atmospheric Implications, *The Journal of Physical Chemistry A*, 117(24), 5117–5123, doi:10.1021/jp4026267, 2013.
- Kameel, F. R., Riboni, F., Hoffmann, M. R., Enami, S. and Colussi, A. J.: Fenton Oxidation of Gaseous Isoprene on Aqueous Surfaces, *The Journal of Physical Chemistry C*, 140725063829009, doi:10.1021/jp505010e, 2014.
- Kawamura, K., Kasukabe, H. and Barrie, L. A.: Secondary formation of water-soluble organic acids and α -dicarbonyls and their contributions to total carbon and water-soluble organic carbon: Photochemical aging of organic aerosols in the Arctic spring, *J. Geophys. Res.*, 115(D21), D21306, doi:10.1029/2010JD014299, 2010.
- Legrand, M., Preunkert, S., Oliveira, T., Pio, C. A., Hammer, S., Gelencsér, A., Kasper-Giebl, A. and Laj, P.: Origin of C2–C5 dicarboxylic acids in the European atmosphere inferred from year-round aerosol study conducted at a west-east transect, *J. Geophys. Res.*, 112(D23), D23S07, doi:10.1029/2006JD008019, 2007.
- Liu, P. S. K., Deng, R., Smith, K. A., Williams, L. R., Jayne, J. T., Canagaratna, M. R., Moore, K., Onasch, T. B., Worsnop, D. R. and Deshler, T.: Transmission Efficiency of an Aerodynamic Focusing Lens System: Comparison of Model Calculations and Laboratory Measurements for the Aerodyne Aerosol Mass Spectrometer, *Aerosol Science and Technology*, 41(8), 721–733, doi:10.1080/02786820701422278, 2007.
- Liu, Y., Siekmann, F., Renard, P., El Zein, A., Salque, G., El Haddad, I., Temime-Roussel, B., Voisin, D., Thissen, R. and Monod, A.: Oligomer and SOA formation through aqueous phase

- photooxidation of methacrolein and methyl vinyl ketone, *Atmospheric Environment*, 49, 123–129, doi:10.1016/j.atmosenv.2011.12.012, 2012.
- Miyakawa, T., Matsuzawa, R., Katayama, M. and Takegawa, N.: Reconsidering Adhesion and Bounce of Submicron Particles Upon High-Velocity Impact, *Aerosol Science and Technology*, 47(5), 472–481, doi:10.1080/02786826.2013.763895, 2013.
- Murray, K. K., Boyd, R. K., Eberlin, M. N., Langley, G. J., Li, L. and Naito, Y.: Definitions of terms relating to mass spectrometry (IUPAC Recommendations 2013), *pac*, 85(7), 1515–1609, doi:10.1351/PAC-REC-06-04-06, 2013.
- Odian, G. G.: Principles of polymerization, Wiley, Hoboken, N.J. [online] Available from: <http://public.eblib.com/EBLPublic/PublicView.do?ptiID=469767> (Accessed 10 October 2014), 2004.
- Renard, P., Siekmann, F., Gandolfo, A., Socorro, J., Salque, G., Ravier, S., Quivet, E., Clément, J.-L., Traikia, M., Delort, A.-M., Voisin, D., Vuitton, V., Thissen, R. and Monod, A.: Radical mechanisms of methyl vinyl ketone oligomerization through aqueous phase OH-oxidation: on the paradoxical role of dissolved molecular oxygen, *Atmospheric Chemistry and Physics*, 13(13), 6473–6491, doi:10.5194/acp-13-6473-2013, 2013.
- Tan, Y., Carlton, A. G., Seitzinger, S. P. and Turpin, B. J.: SOA from methylglyoxal in clouds and wet aerosols: Measurement and prediction of key products, *Atmospheric Environment*, 44(39), 5218–5226, doi:10.1016/j.atmosenv.2010.08.045, 2010.
- Zhang, X., Chen, Z. M. and Zhao, Y.: Laboratory simulation for the aqueous OH-oxidation of methyl vinyl ketone and methacrolein: significance to the in-cloud SOA production, *Atmospheric Chemistry and Physics*, 10(19), 9551–9561, doi:10.5194/acp-10-9551-2010, 2010.

Referee 2

Interactive comment on “Aqueous phase oligomerization of methyl vinyl ketone through photooxidation – Part 1: Aging processes of oligomers” by P. Renard et al.

RC C4754: 'Review of interesting and novel study by Renard et al.', Anonymous Referee #2, 12 Jul 2014

The authors appreciate many important comments raised by Reviewer 2 which have been considered in the new version of the manuscript. The authors' answers to the questions/comments of Reviewer 2 are presented below.

Question:

1. The language in the manuscript is sometimes awkward and there are numerous errors in English language grammar and syntax. These include singular/plural disagreements between nouns and verbs, improper choice of prepositions, missing subjects, etc.... The manuscript should be edited for language before acceptance for publication.

Answer:

Done.

Question:

2. p. 15287, line 12: change "ionic" to "ion"

Answer:

Done.

Question:

3. p. 15288, line 13: define "UPLC"

Answer:

Done.

Question:

4. p. 15288, line 4: The authors state that the experimental conditions in Table 1 were chosen to be representative of cloud droplets or wet aerosol conditions. While the lowest MVK concentration (200 μM) might represent total WSOC concentrations in some clouds or fogs, it is unlikely to find such high concentrations of a single ketone. The minimum concentration of H_2O_2 (4000 μM) is also much higher than seen in ambient clouds or fogs, where reported observations are generally at least 10x lower. Based on these discrepancies, I would conclude that the lowest MVK and H_2O_2 concentrations are perhaps an order of magnitude or so higher than in ambient clouds and fogs. This should be clarified for the reader.

Answer:

In the comparison between our experimental concentrations with atmospheric ones, MVK is considered a proxy for UWSOC. We do not intend to compare the H_2O_2 concentrations with the atmospheric ones (as H_2O_2 is not the only source of atmospheric $\cdot\text{OH}$), but we compare the estimated $\cdot\text{OH}$ concentrations with the atmospheric ones. We modified the text accordingly, it now reads:

“Tan et al. (2010) and Renard et al. (2013) have shown the important impact of initial concentrations on oligomer formation. The experiments were thus carried out with various MVK initial concentrations (Table 1), i.e., 0.2, 0.5, 2, 5 and 20 mM (corresponding to 9.6 to 960 mgC L^{-1}). Considering MVK as a proxy for UWSOC, this concentration range is comprised in the range of the estimated total UWSOC concentrations from fog droplets to wet aerosol (Renard et al., 2013).

The initial H_2O_2 concentrations were chosen in order to obtain a ratio ($\frac{[\text{H}_2\text{O}_2]_0}{[\text{MVK}]_0} = 20$), in order to favor $\cdot\text{OH}$ reaction with MVK rather than with H_2O_2 by more than 90 %. Under these conditions, $\cdot\text{OH}$ concentrations were estimated in the range $(2 - 6) \times 10^{-14}$ M (Supplementary information SI3), which falls in the range of the estimated values for $\cdot\text{OH}$ concentrations in cloud and fog droplets (Herrmann et al., 2010; Ervens and Volkamer, 2010 and Arakaki et al., 2013).”

Question:

5. p. 12588, line 14: How were OH concentrations estimated? Were they measured in solution, e.g., by adding a "clock" species with a known OH-rxn rate?

Answer:

•OH concentrations were calculated by means of two different methods (methods a) and b) below), which gave similar results, as shown hereafter. These calculations were added in the supplementary information of the new version of the manuscript.

a) Considering reactions R1 to R3, •OH concentrations were calculated assuming the steady state approximation at time 0:

$$[OH] = \frac{2 \times J_{H_2O_2} \times [H_2O_2]}{k_3 \times [MVK] + k_2 \times [H_2O_2]}$$



$J_{H_2O_2}$ was determined by fitting H_2O_2 concentration decay



$$k_2 = 2,95 \cdot 10^7 \text{ M}^{-1} \text{ s}^{-1} \text{ at } 25^\circ \text{ C} \quad (\text{Christensen et al., 1982})$$



$$k_3 = 7.3(\pm 0,5) 10^9 \text{ M}^{-1} \text{ s}^{-1} \text{ at } 25^\circ \text{ C} \quad (\text{Schöne et al., 2014})$$

The obtained values are $[\cdot OH] = (5 - 6) \times 10^{-14} \text{ M}$ for pH 3 - 6

b) Fitting the initial MVK decay with an exponential decay:

$$[MVK]_t = [MVK]_0 \times e^{-(k_3 \times [\cdot OH] \times t)}$$

With $k_3 = 7.3 (\pm 0,5) 10^9 \text{ M}^{-1} \text{ s}^{-1}$ at 25° C (Schöne et al., 2014), we obtain similar values for •OH steady state concentrations ($[\cdot OH] = 2 \times 10^{-14} \text{ M}$) as for the previous estimation.

Question:

6. p. 15288, line 23: change "its resolution mode" to "its high resolution mode"

7. p. 15289: What mass accuracy was achieved for the instrument?

Answer:

The term “resolution mode” is used by the instrument constructor to specify V-mode acquisition, corresponding to a resolution of 18,000 FWHM (Full width at half maximum) at m/z 400. The term “high resolution mode” corresponds to the W-mode acquisition, with a resolution of 40,000 FWHM at m/z 400. We only used the first mode. The mass accuracy was < 5 ppm. The text has been modified to make these explanations clearer. The text now reads:

“The mass spectrometer was used in its resolution mode (V-mode), up to 18,000 FWHM (Full width at half maximum) at m/z 400. The mass accuracy was < 5 ppm, and allowed for the determination of elemental composition of organic species (Renard et al., 2013 and Renard et al., 2014).”

Question:

8. p. 15290, lines 1-3: Given that the 211 nm absorption is proportional to the sum of the H₂O₂ and MVK concentrations, it is unclear to me how measuring at this wavelength defines the MVK oxidation rate. Please clarify. Presumably you need the combination of the K and R bands to separate changes in MVK and H₂O₂ concentrations.

Answer:

The instrument described in the paragraph (UHPLC-UV) allows for a chromatographic separation of MVK and H₂O₂ prior detection by UV absorbance: H₂O₂ has a retention time of 0.5 minutes and is chromatographically separated from MVK which has a retention time of 1.8 minutes. We modified the text to clarify this point. Furthermore, some Tables and Figures (Table 1, Figure 2a, Figure 6) have been slightly modified using more appropriate calibrations of H₂O₂ and MVK concentrations by UHPLC-UV analysis. The chromatograms were monitored at 270, 229 nm and 211 nm and the peak areas were found to be directly proportional to both the H₂O₂ and the MVK concentrations in the range of the studied concentrations: at 211 nm for low MVK concentrations ($[MVK] \leq 2$ mM), at 229 nm for low H₂O₂ concentrations and for high concentrations of MVK ($[H_2O_2] < 40$ mM and $2 < [MVK] \leq 20$ mM), and at 270 nm for higher concentrations of H₂O₂ (up to 400 mM). The whole paragraph 2.2.2 now reads:

“An ultra-high performance liquid chromatographic (UHPLC) system (ThermoScientific, Accela 600 auto sampler and Accela 600 pump) coupled to a diode array detector (ThermoScientific, Accela 600 PDA detector) was used to monitor the concentrations of MVK and H₂O₂ sampled from the photoreactor. The chromatographic separation was performed using a column (ThermoScientific, Hypersil GOLD, 100 x 2.1 mm - 1.9 μm) at 40°C and a flow rate of 300 μL min⁻¹. The mobile phase was water/acetonitrile (98:2) (v/v) and the injection volume was set to 2 μL. The spectra were recorded from 200 to 360 nm.

Under these conditions, H₂O₂ has a retention time of 0.5 min and is chromatographically separated from MVK which has a retention time of 1.8 minutes. The UV spectrum of aqueous H₂O₂ exponentially increases with decreasing wavelength, it becomes intense below 300 nm. Aqueous solutions of MVK show an intense absorption band (K-band; π → π transition) that peaks at 211 nm and a weak absorption band (R-band; n → π* transition) that peaks at 308 nm. The chromatograms were monitored at 270, 229 nm and 211 nm and the peak areas were found to be directly proportional to both the H₂O₂ and the MVK concentrations in the range of the studied concentrations: at 211 nm for low MVK concentrations ([MVK] ≤ 2 mM), at 229 nm for low H₂O₂ concentrations and for high concentrations of MVK ([H₂O₂] < 40 mM and 2 < [MVK] ≤ 20 mM), and at 270 nm for higher concentrations of H₂O₂ (up to 400 mM).”*

Question:

9. p. 15290, line 24: Please give the manufacturer for the TOC/TN instrument.

Answer:

Done: the text now reads:

“A total organic carbon / total nitrogen (TOC/TN) analyzer (Analytik Jena, N/C2100S) with the non-purgeable organic carbon (NPOC) method was used to quantify the produced oligomers in our liquid samples.”

Question:

10. p. 15291: Please clarify use of the NPOC measurement mode for TOC. Using this mode on acidified samples should eliminate small molecules, including low MW carboxylic acids.

That seems useful if you want to quantify the OC that will be released as OA upon drop evaporation. Is that the intent?

Answer:

Prior TOC measurements, MVK and small and/or volatile reactants and reaction products were specifically removed from the samples by preparative liquid chromatography. We modified the paragraph in order to clarify this point. The whole paragraph 2.2.4 now reads:

“TOC measurements were associated to preparative liquid chromatography to separate the oligomers from the small and/or volatile reactants and reaction products in the liquid samples, in order to measure the oligomer mass yields in experiment A (see section 3.2.3). A total organic carbon / total nitrogen (TOC/TN) analyzer (Analytik Jena, N/C2100S) with the non-purgeable organic carbon (NPOC) method was used to quantify the produced oligomers in our liquid samples.

The NPOC method consists in pre-purging samples with oxygen and pre-acidifying (at pH=2 with HCl) to remove the inorganic carbon and purgeable organic carbon. TOC is measured by injecting the sample into a heated combustion tube (800°C) with an oxidation catalyst. The CO₂ produced is measured by a non-dispersive infrared (NDIR) gas analyzer. TN is measured in parallel using chemiluminescence detection (CLD).”

Question:

11. Accurate quantification of the CO₂⁺ fragment in the AMS requires good information about the CO₂ concentration in the sample air stream. How was this quantified? Indoor CO₂ concentrations can be much higher than outdoor concentrations.

Answer:

The AMS samples particles more efficiently than gases by 7 orders of magnitude (Allan et al., 2003; Cubisson et al., 2011). It follows that gaseous CO₂ at a concentration of 1000 ppm (indoor air level, (Hussin et al., 2014) is expected to generate 100 ng m⁻³ of equivalent aerosol signal at m/z 44. This interference needs to be accounted for in view of the low aerosol equivalent signal measured at this specific ion in our experiments (Figure 3, maximum aerosol signal at CO₂⁺ of 4

$\mu\text{g m}^{-3}$). Accordingly, mass spectra of filtered air (using a HEPA capsule filter) were taken prior each series of nebulizing experiments in order to adjust the m/z 44 entry of the fragmentation table due to gas phase CO_2 .

The text has been modified accordingly: in section 2.3, the following sentence has been added: “*Mass spectra of filtered air (using a HEPA capsule filter) were taken prior each series of nebulizing experiments in order to adjust the m/z 44 entry of the fragmentation table due to gas phase CO_2 .*”

Question:

12. p. 15293, lines 14-15: Why were these fragments "thought to be" $\text{C}_2\text{H}_3\text{O}^+$ and CO_2^+ ? Aren't you using the high res AMS data where these ions are distinguished from other ions with the same unit mass?

Answer:

Yes, this is right. For the analysis of the HR-ToF-AMS spectra and identification of the respective ions, we used the high resolution V-mode (up to 2000 at m/z 200). Therefore, we can clearly identify $\text{C}_2\text{H}_3\text{O}^+$ and CO_2^+ ions fragments. The text has been modified accordingly in the new version of the manuscript, it now reads:

- **In section 2.3:** “*The instrument was used under standard conditions (vaporizer at 600°C and electron ionization at 70 eV), in the high sensitivity V-mode (up to 2000 at m/z 200).*”
- **In section 3.1.2:** “*The AMS mass spectra (Figure 3) show two dominant fragments, at m/z 43 and m/z 44 (corresponding to $\text{C}_2\text{H}_3\text{O}^+$ and CO_2^+ fragments).*”

Question:

13. p. 15293, line 28: the second ion listed here should be m/z 44.

Answer:

Done.

Question:

14. p. 15294, line 10: The AMS collection efficiencies stated (0.07 to 0.21) seem very small for organic aerosols. Please comment on these values relative to those typically reported for OA in other AMS studies.

Answer:

The AMS collection efficiencies were investigated by comparing AMS to SMPS measurements. The AMS collection efficiency (CE) represents the efficiency with which particles are transmitted through the aerodynamic lens system and the particle time-of-flight (PToF) chamber, as well as the bouncing effect on the vaporizer surface (Huffman et al., 2005, Docherty et al., 2013). It is thus likely that the physical and chemical properties of our particles induced a low transmission and/or a high bouncing effect. In addition to these effects, it is possible that our low CE values (compared to chamber studies or ambient aerosols) were also due to the particle size range (50 nm - 150 nm mass distribution), as the lowest part of this size range corresponds to the region where the AMS transmission curve varies greatly (Liu et al., 2007). This effect is confirmed by the fact that our lowest values of CE (0.07) were obtained for the lowest MVK initial concentrations (0.2 – 2 mM) where the smallest particles were formed (50 nm mass distribution).

The text (in section 3.1.2) has been modified accordingly, it now reads: *“For the quantitative study (section 3.2), we used the data provided by the SMPS analysis. Note that the overall collection efficiencies (CE) of the AMS in our experiments varied from 0.07 to 0.21 (related to the SMPS signal). These low CE values (compared to chamber studies or ambient aerosols) can be due to particle bounce at the vaporizer surface before volatilization and to the shape and size-dependent transmission of the aerodynamic lens. As a result, the studied compounds did not volatilize sufficiently fast at standard AMS vaporizer temperatures to be fully detected (Liu et al., 2007; Docherty et al., 2013; Miyakawa et al., 2013). In addition to these effects, it is possible that our low CE values were also due to the particle size range (50 nm - 150 nm mass distribution), as the lowest part of this size range corresponds to the region where the AMS transmission curve varies greatly (Liu et al., 2007). This effect is confirmed by the fact that our lowest values for CE (0.07) were obtained for the lowest MVK initial concentrations (0.2 – 2 mM) where the smallest particles were formed (50 nm mass distribution).”*

Question:

15. p. 15294, line 22: please change "increasing mode" to "increasing mode size"

Answer:

Done.

Question:

16. p. 15296 and elsewhere: The authors need to comment on the possible role of OA concentration in altering the fraction of organic matter that partitions to the aerosol phase. The lower concentration experiments could have lower SOA yields, in part, because at lower OA concentrations a bigger fraction of the organic matter resides in the gas phase. This partitioning effect could also alter the relative oxygenation of the OA produced since only the lowest vapor pressure products will enter the particle phase when OA concentrations are low.

Answer:

It is true that the OA concentrations certainly influence their gas/particle partitioning in our set up, even if the residence time is of the order of a minute. However, looking at the data in Tables 2 and 3, it is not possible to observe any significant evolution in the obtained SOA mass yields, due to their large uncertainties. This is the reason why a different experiment was performed using preparative chromatography and TOC analysis that gave the oligomer mass yield with a much smaller uncertainty. However, this check was done only for one experiment (exp A), so it is not possible to deduce any SOA mass yield evolution from our results.

In contrast, the O/C and H/C ratios clearly show statistically stable values when the total particle mass increases from 100 to 900 $\mu\text{g}/\text{m}^3$ (Table 3). It is thus likely that the total mass loading does not influence the relative oxygenation of the OA produced under our experimental conditions.

In order to make these points clearer in the manuscript, we have modified the beginning of section 3.23, it now reads:

“The SOA mass yields, Y_t , were calculated at each reaction time step t from eq. 2.

$$Y_t = \frac{[SOA]_t}{\Delta[MVK]_t} \quad (eq. 2)$$

Where $\Delta[MVK]_t$ is the consumed $[MVK]$ in mg L^{-1} at reaction time t ; and $[SOA]_t$ is the formed SOA mass at reaction time t , in mg per L of evaporated water. This term takes into account the SOA mass (M_{SMPS}) measured by the SMPS at time t (in $\mu\text{g m}^{-3}$), the atomizer flow ($F_{atomizer}$ in L m^{-3}), the dilution (f_{dil}), and the transmission efficiency in our nebulizing system (T_{eff} in %) (see Table S1).

$$[SOA]_t = \frac{M_{SMPS} \times T_{eff}}{F_{atomizer} \times f_{dil} \times 1000} \quad (\text{eq. 3})$$

The yields obtained at t_{max} for experiments A, B and C are shown in Table 3. Although the total SOA mass (at t_{max}) increases linearly with the initial concentration for these three experiments, the yields are statistically identical as well as their H/C and O/C ratios. Due to the very large uncertainties affected to our yield determinations (see below), it is not possible to use these data (Table 2 and 3) to provide any interpretation on the possible effect of initial concentrations on the yields. In contrast, the O/C and H/C ratios clearly show statistically stable values when the total particle mass increases from 100 to 900 $\mu\text{g/m}^3$ (Table 3). It is thus likely that the total mass loading does not influence the relative oxygenation of the SOA produced (at t_{max}) under our experimental conditions.

Although the particle mass loadings (M_{SMPS}) were accurately measured, our yield determinations were affected by large uncertainties due to the estimation of the transmission efficiency in our nebulizing system (see supplementary information 1).”

Question:

17. pp. 15297-15298: The authors do a nice job talking about the changes in chemistry and SOA yield as a function of oxidation time. This discussion, however, would benefit from tying it back to the ambient atmosphere. Please discuss what yield/time is most relevant for typical atmospheric conditions.

Answer:

The transfer of these results to atmospheric conditions is the scope of part 2 of this study where they have been included in a multiphase atmospheric model (Ervens et al., 2014). Briefly, the model results indicate that cloud conditions would allow for the formation of very few oligomers, while in wet aerosol conditions, oligomer concentrations would increase up to 250 ng m^{-3} within 350 min. The comparison of predicted oligomer formation shows that for most model

assumptions (e.g. depending on the assumed partitioning of MVK and MACR), SOA formation from isoprene in the gas phase would exceed aqueous SOA formation by a factor 3–4.

Question:

18. p. 15298, line 2: I think the percentage here should be 70 +/- 50%

Answer:

Yes, this was a typo.

Question:

19. Fig. 8: The time evolution of the experiments needs to be better displayed in this figure.

Answer:

Done.

Question:

20. p. 15302, line 1: change "ones" to "compounds"

Answer:

Done.

Question:

21. p. 15302, lines 2-3: This sentence is missing a subject. Latter is an adjective. Latter what...?

Answer:

According to this comment and those by other reviewers, the whole paragraph has been modified. It now reads: *“Considering the results obtained here on oligomer formation and aging from MVK at varying initial concentrations together with those obtained by previous studies on the identification of the low-molecular-weight compounds products of the reaction (Zhang et al., 2010), a general scheme of the potential atmospheric fate of MVK in the aqueous phase is shown*

on Figure 11. MVK $\dot{\text{O}}\text{H}$ -oxidation undergoes kinetic competition between functionalization and oligomerization, depending on the precursor initial concentration. At 2 mM of MVK and above this concentration, oligomerization dominates over functionalization. At these concentrations, $\dot{\text{O}}\text{H}$ -oxidation of MVK forms oligomers that are SV-OOA, with low O/C (lower than 0.50) and high f_{43} . Oligomers are then fragmented, via unidentified intermediates that have the properties of LV-OOA (with increasing O/C and decreasing H/C, Figure 9) which then form organic diacids. For lower initial MVK concentrations (< 2 mM), oligomerization is not the major process, and functionalization dominates, ending into small carbonyls, dicarbonyls and acids that were identified by Zhang et al., (2010) (Figure 11).

Among the atmospherically relevant alkenoic alcohols, acids, ketones and aldehydes (i.e. UWSOC), although MVK is one of the most abundant species, it is one of the most volatile ($P_{\text{sat}} = 10^{-5} - 0.1$ atm, with $P_{\text{sat}(\text{MVK})} = 0.1$ atm at 25°C ; Asher and Pankow 2006), and one of the least soluble compounds ($K_{\text{H}} = 1 - 10^3$ M atm $^{-1}$, with $K_{\text{H}(\text{MVK})} = 41$ M atm $^{-1}$ at 25°C ; Iraci et al., 1999). The atmospheric impacts of the processes shown here should thus be very limited for MVK alone. However, the oligomerization mechanism undergone by MVK occurs via saturation of the vinyl group (Renard et al., 2013), and the resulting radical monomer is stabilized by the resonance effect with the adjacent carbonyl group thus decreasing the enthalpy of polymerization facilitating the oligomerization in the aqueous phase compared to other molecules. More generally, conjugation of the C=C with substituents such as the benzene ring (styrene and *a*-methylstyrene), and alkene double bond (butadiene and isoprene), the carbonyl linkage (acrylic acid, methyl acrylate, methyl methacrylate), and the nitrile group (acrylonitrile) similarly leads to stabilization of the monomer and decreases enthalpies of polymerization (O'dian 2004). It is thus likely that a large number of atmospherically relevant molecules can follow the same process either in the bulk or at the wet aerosol interface (Kameel et al., 2013; Kameel et al., 2014). In this context, our results suggest that this class of compounds can impact the aerosol composition, and contribute to aqSOA formation upon water evaporation. The corresponding aqSOA mass yields seem to depend on the spectral irradiance of the light used to initiate the photochemistry, but further studies are needed to confirm this point. Finally, the aging of the oligomers formed could be an explanation (at least in part) for the presence the diacids (such as oxalic, malonic and succinic acids) observed in the ambient aerosol (Legrand et

al., 2007; Kawamura et al., 2010). In Part 2 of this study, the atmospheric relevance of these processes is explored by means of multiphase box model studies.”

References:

- Allan, J. D., Jimenez, J. L., Williams, P. I., Alfarra, M. R., Bower, K. N., Jayne, J. T., Coe, H. and Worsnop, D. R.: Quantitative sampling using an Aerodyne aerosol mass spectrometer 1. Techniques of data interpretation and error analysis, *J. Geophys. Res.*, 108(D3), 4090, doi:10.1029/2002JD002358, 2003.
- Arakaki, T., Anastasio, C., Kuroki, Y., Nakajima, H., Okada, K., Kotani, Y., Handa, D., Azechi, S., Kimura, T., Tsuchi, A. and Miyagi, Y.: A General Scavenging Rate Constant for Reaction of Hydroxyl Radical with Organic Carbon in Atmospheric Waters, *Environmental Science & Technology*, 130718140737000, doi:10.1021/es401927b, 2013.
- Asher, W. E. and Pankow, J. F.: Vapor pressure prediction for alkenoic and aromatic organic compounds by a UNIFAC-based group contribution method, *Atmospheric Environment*, 40(19), 3588–3600, doi:10.1016/j.atmosenv.2005.12.004, 2006.
- Christensen, H., Sehested, K. and Corfitzen, H.: Reactions of hydroxyl radicals with hydrogen peroxide at ambient and elevated temperatures, *J. Phys. Chem.*, 86(9), 1588–1590, doi:10.1021/j100206a023, 1982.
- Cubison, M. J., Ortega, A. M., Hayes, P. L., Farmer, D. K., Day, D., Lechner, M. J., Brune, W. H., Apel, E., Diskin, G. S., Fisher, J. A., Fuelberg, H. E., Hecobian, A., Knapp, D. J., Mikoviny, T., Riener, D., Sachse, G. W., Sessions, W., Weber, R. J., Weinheimer, A. J., Wisthaler, A. and Jimenez, J. L.: Effects of aging on organic aerosol from open biomass burning smoke in aircraft and laboratory studies, *Atmos. Chem. Phys.*, 11(23), 12049–12064, doi:10.5194/acp-11-12049-2011, 2011.
- Docherty, K. S., Jaoui, M., Corse, E., Jimenez, J. L., Offenberg, J. H., Lewandowski, M. and Kleindienst, T. E.: Collection Efficiency of the Aerosol Mass Spectrometer for Chamber-Generated Secondary Organic Aerosols, *Aerosol Science and Technology*, 47(3), 294–309, doi:10.1080/02786826.2012.752572, 2013.
- Ervens, B., Renard, P., Ravier, S., Clément, J.-L. and Monod, A.: Aqueous phase oligomerization of methyl vinyl ketone through photooxidation– Part 2: Development of the chemical mechanism and atmospheric implications, *Atmos. Chem. Phys. Discuss*, 14, 21565–21609, doi:10.5194/acpd-14-21565-2014, 2014.
- Ervens, B. and Volkamer, R.: Glyoxal processing by aerosol multiphase chemistry: towards a kinetic modeling framework of secondary organic aerosol formation in aqueous particles, *Atmospheric Chemistry and Physics*, 10(17), 8219–8244, doi:10.5194/acp-10-8219-2010, 2010.
- Herrmann, H., Hoffmann, D., Schaefer, T., Brüner, P. and Tilgner, A.: Tropospheric Aqueous-Phase Free-Radical Chemistry: Radical Sources, Spectra, Reaction Kinetics and Prediction Tools, *ChemPhysChem*, 11(18), 3796–3822, doi:10.1002/cphc.201000533, 2010.
- Huffman, J. A., Jayne, J. T., Drewnick, F., Aiken, A. C., Onasch, T., Worsnop, D. R. and Jimenez, J. L.: Design, Modeling, Optimization, and Experimental Tests of a Particle Beam Width Probe for the Aerodyne Aerosol Mass Spectrometer, *Aerosol Science and Technology*, 39(12), 1143–1163, doi:10.1080/02786820500423782, 2005.

- Hussin, M., Ismail, M. R. and Ahmad, M. S.: Air-conditioned university laboratories: Comparing CO₂ measurement for centralized and split-unit systems, *Journal of King Saud University - Engineering Sciences*, doi:10.1016/j.jksues.2014.08.005, 2014.
- Iraci, L. T., Baker, B. M., Tyndall, G. S. and Orlando, J. J.: Measurements of the Henry's law coefficients of 2-methyl-3-buten-2-ol, methacrolein, and methylvinyl ketone, *Journal of atmospheric chemistry*, 33(3), 321–330, 1999.
- Kameel, F. R., Hoffmann, M. R. and Colussi, A. J.: OH Radical-Initiated Chemistry of Isoprene in Aqueous Media. Atmospheric Implications, *The Journal of Physical Chemistry A*, 117(24), 5117–5123, doi:10.1021/jp4026267, 2013.
- Kameel, F. R., Riboni, F., Hoffmann, M. R., Enami, S. and Colussi, A. J.: Fenton Oxidation of Gaseous Isoprene on Aqueous Surfaces, *The Journal of Physical Chemistry C*, 140725063829009, doi:10.1021/jp505010e, 2014.
- Kawamura, K., Kasukabe, H. and Barrie, L. A.: Secondary formation of water-soluble organic acids and α -dicarbonyls and their contributions to total carbon and water-soluble organic carbon: Photochemical aging of organic aerosols in the Arctic spring, *Journal of Geophysical Research*, 115(D21), doi:10.1029/2010JD014299, 2010.
- Legrand, M., Preunkert, S., Oliveira, T., Pio, C. A., Hammer, S., Gelencsér, A., Kasper-Giebl, A. and Laj, P.: Origin of C₂–C₅ dicarboxylic acids in the European atmosphere inferred from year-round aerosol study conducted at a west-east transect, *J. Geophys. Res.*, 112(D23), D23S07, doi:10.1029/2006JD008019, 2007.
- Liu, P. S. K., Deng, R., Smith, K. A., Williams, L. R., Jayne, J. T., Canagaratna, M. R., Moore, K., Onasch, T. B., Worsnop, D. R. and Deshler, T.: Transmission Efficiency of an Aerodynamic Focusing Lens System: Comparison of Model Calculations and Laboratory Measurements for the Aerodyne Aerosol Mass Spectrometer, *Aerosol Science and Technology*, 41(8), 721–733, doi:10.1080/02786820701422278, 2007.
- Miyakawa, T., Matsuzawa, R., Katayama, M. and Takegawa, N.: Reconsidering Adhesion and Bounce of Submicron Particles Upon High-Velocity Impact, *Aerosol Science and Technology*, 47(5), 472–481, doi:10.1080/02786826.2013.763895, 2013.
- Odian, G. G.: Principles of polymerization, Wiley, Hoboken, N.J. [online] Available from: <http://public.eblib.com/EBLPublic/PublicView.do?ptiID=469767> (Accessed 10 October 2014), 2004.
- Renard, P., Reed Harris, A. E., Rapf, R. J., Ravier, S., Demelas, C., Coulomb, B., Quivet, E., Vaida, V. and Monod, A.: Aqueous Phase Oligomerization of Methyl Vinyl Ketone by Atmospheric Radical Reactions, *The Journal of Physical Chemistry C* [online] Available from: <http://pubs.acs.org/doi/abs/10.1021/jp5065598> (Accessed 23 October 2014), 2014.
- Renard, P., Siekmann, F., Gandolfo, A., Socorro, J., Salque, G., Ravier, S., Quivet, E., Clément, J.-L., Traikia, M., Delort, A.-M., Voisin, D., Vuitton, V., Thissen, R. and Monod, A.: Radical mechanisms of methyl vinyl ketone oligomerization through aqueous phase OH-oxidation: on the paradoxical role of dissolved molecular oxygen, *Atmospheric Chemistry and Physics*, 13(13), 6473–6491, doi:10.5194/acp-13-6473-2013, 2013.
- Schöne, L., Schindelka, J., Szeremeta, E., Schaefer, T., Hoffmann, D., Rudzinski, K. J., Szmigielski, R. and Herrmann, H.: Atmospheric aqueous phase radical chemistry of the

isoprene oxidation products methacrolein, methyl vinyl ketone, methacrylic acid and acrylic acid – kinetics and product studies, *Physical Chemistry Chemical Physics*, 16(13), 6257, doi:10.1039/c3cp54859g, 2014.

Tan, Y., Carlton, A. G., Seitzinger, S. P. and Turpin, B. J.: SOA from methylglyoxal in clouds and wet aerosols: Measurement and prediction of key products, *Atmospheric Environment*, 44(39), 5218–5226, doi:10.1016/j.atmosenv.2010.08.045, 2010.

Zhang, X., Chen, Z. M. and Zhao, Y.: Laboratory simulation for the aqueous OH-oxidation of methyl vinyl ketone and methacrolein: significance to the in-cloud SOA production, *Atmospheric Chemistry and Physics*, 10(19), 9551–9561, doi:10.5194/acp-10-9551-2010, 2010.

Referee 3

Interactive comment on “Aqueous phase oligomerization of methyl vinyl ketone through photooxidation – Part 1: Aging processes of oligomers” by P. Renard et al.

RC C4779: 'Review of Renard et al.', Anonymous Referee #3, 13 Jul 2014 Printer-friendly Version

The authors appreciate many important comments raised by Reviewer 3 which have been considered in the new version of the manuscript. The authors' answers to the questions/comments of Reviewer 3 are presented below.

Question 1:

Overall, the writing quality is not strong. As examples:

i. An Abstract should be a clear, succinct description of the experiments and results, and so the first paragraph should be removed.

Answer:

The abstract was modified according to the reviewer's comment as well as those of other reviewers, it now reads:

“It has recently been established that unsaturated water soluble organic compounds (UWSOC) might efficiently form oligomers in polluted fogs and wet aerosol particles, even for weakly soluble ones like methyl vinyl ketone (MVK). The atmospheric relevance of these processes is explored by means of multiphase process model studies (in a companion paper). In the present study, we investigate the aging of these aqueous phase MVK-oligomers formed via OH-oxidation, as well as their ability to form secondary organic aerosol (SOA) upon water evaporation. The comparison between aqueous phase composition and aerosol composition after nebulization of the corresponding solutions shows similar trends for oligomer formation and aging. The measurements reveal that oligomer aging leads to the formation of organic diacids. Quantification of the SOA mass formed after nebulization is performed, and the obtained SOA mass yields seem to depend on the spectral irradiance of the light used to initiate the

photochemistry. Investigating a large range of initial MVK concentrations (0.2 – 20 mM), the results show that its \cdot OH-oxidation undergoes a kinetic competition between functionalization and oligomerization that is dependent on the precursor concentration. At high initial MVK concentrations ($\geq 2\text{mM}$), oligomerization prevails over functionalization, while at lower initial concentrations, oligomerization is not the major process, and functionalization dominates, resulting in small carbonyls, dicarbonyls and monoacids. The atmospheric implications of these processes are discussed.”

ii. The Results section simply lists the results one after the other, without connecting one section to the others, i.e. helping the reader to better understand the work,

Answer:

The manuscript has been modified according to this comment: each part of the results has been introduced by a small paragraph.

iii. The Discussion section starts immediately with some highly detailed discussion without codifying the overall results from the study.

Answer:

The manuscript has been modified according to this comment:

- The discussion section is now introduced by the following paragraph:

“This section discusses the results obtained on the aging of the reaction products of MVK- \cdot OH experiments and the related oxidation processes by two relevant ways. First, the competition between functionalization and oligomerization and the subsequent aging according to the initial concentration of MVK is discussed; and second, a Van Krevelen diagram (i.e, H/C vs O/C ratios) of the obtained SOA is presented and compared to previous studies.”

- Section 4.1 is now introduced by the following paragraph:

“In order to compare our work with the aging of organic aerosol in the atmosphere compiled by Ng et al. (2010), we used the AMS data, and in particular, the development of the two dominant fragments, m/z 44 (CO_2^+) and m/z 43 (mostly $\text{C}_2\text{H}_3\text{O}^+$), observed in our study. More precisely, we focused on the ratio of m/z 44 and m/z 43 to total organic aerosol, f_{44} and f_{43} , respectively.”

iv. The Figures have too small labels and axis values.

Answer:

The labels and axis values have been enlarged in the new version of the manuscript.

References: Please check that all relevant studies related to oligomerization have been included. For example, the work of Aljawhary et al., AMT, 2013 describes the loss, presumably by OH oxidation, of SOA oligomers in solution.

Answer:

This reference was added as well as other recent works on radical oligomerisation, such as Kameel et al. (2013); Kameel et al. (2014); Daumit et al. (2014); Tan et al. (2012); Zhao et al., (2012).

Question 2:

The authors need to address how the sensitivity of ESI to different classes of compounds affects their results. For example, in Figure 2 how much of the change in shape of the spectrum is due to the formation of polyacids that are detected easily by ESI, when starting with a precursor that does not contain an acid functionality? Are oligomers detected as efficiently as the monomers?

Answer:

The ESI source used in this study is designed to operate with UPLC which requires very high column pressure ($\sim 10^4$ PSI), and thus necessitates, in the ESI, high flows of desolvation gas (N_2 at 800 L h^{-1}). As a result, most of the small and/or volatile molecules are lost prior entering the mass spectrometer. For example, the instrument can barely detect MVK, oxalic and pyruvic

acids (m/z 71⁺ 89⁻ and 87⁻, respectively). Conversely, a higher signal is obtained for larger molecules, identified as MVK-oligomers (Figure 2), by means of the UPLC-ESI-MS used in its resolution mode, up to 18,000 FWHM (Full width at half maximum) at m/z 400. As a result, it is likely that oligomers are detected more efficiently than monomers, which in turn are detected more efficiently than MVK, or small carboxylic acids, but the instrument was not used for quantification. This is the reason why we have performed UHPLC-UV and ion chromatography analyses of the solutions to specifically quantify MVK, H₂O₂ and the formed carboxylic acids.

The manuscript has been modified to clarify this point, as follows:

An introduction has been added to section 2.2, it reads:

“Aliquots of the solution sampled from the photoreactor were analyzed for qualitative structure elucidation of the oligomers using ultra-performance liquid chromatography mass spectrometry (UPLC-ESI-MS); and for quantitative studies of the concentrations of i) MVK and H₂O₂ by liquid chromatography coupled to UV detection (UHPLC-UV), iii) carboxylic acids by ion chromatography-mass spectrometry (IC-ESI-MS), and iv) oligomers using preparative liquid chromatography associated to total organic carbon (TOC) analyses.”

in section 2.1.1,

“The mass spectrometer was used in its resolution mode (V-mode), up to 18,000 FWHM (Full width at half maximum) at m/z 400. The mass accuracy was < 5 ppm, and allowed for the determination of elemental composition of organic species (Renard et al., 2013 and Renard et al., 2014), using the I-FIT software. The I-FIT isotope predictive filtering is a strategy to reduce the number of proposed elemental compositions using algorithms to estimate the number of carbon, oxygen (or sulfur) atoms in an unknown molecule based on the mass of the molecular ion and the relative intensity of the 1st and 2nd isotopes (Hobby, 2005).”

Question 3:

For the AMS spectra in Figure 3, has high resolution mass fitting identified the composition of the different ions labelled? For example, m/z 43 may have multiple elemental compositions.

Answer:

For the analysis of the AMS spectra and identification of the respective ions, we used the high resolution V-mode (up to 2000 at m/z 200). Using this mode with the adapted software PIKA 1.10H for data treatment, we can clearly distinguish between $C_2H_3O^+$ and $C_3H_7^+$ ions at m/z 43. Other ions were not observed at this mass in our experiments. The blue bar in Figure 3 only represents $C_2H_3O^+$ ions.

The manuscript has been modified to clarify this point in section 3.1.2, as follows:

“The AMS mass spectra (Figure 3) show two dominant fragments, at m/z 43 and m/z 44 (corresponding to $C_2H_3O^+$ and CO_2^+ fragments).”

Question 4:

When quantitatively comparing data at different times in the reaction (e.g. AMS data in Figure 4), how is it known that the nebulizer output is constant from one time to the other? Nebulizer outputs are affected by the surface tension and volatility of the solution being atomized. Indeed, the numbers of particles being formed is changing dramatically during the experiment as shown by the SMPS scans in Figure 5. Why is that occurring, for a “constant output” TSI atomizer? How does this affect the interpretation of the results? Should the authors normalize all their aerosol results to the changing number output of the atomizer? Please clarify.

Question 5:

As a related question, if the number output of the atomizer is changing I don't understand how a yield can be quantified. For example, if the number of particles being produced by the atomizer is lower at the beginning of the experiment than at the end, then the yield (using equation 2) will be calculated to be lower. This does not reflect changing chemistry, only the changing efficiency of atomization. Unless I am incorrect, this will make the stated yields invalid.

Answer (4 and 5):

- The AMS mass spectra presented in Figure 4 show normalized signals, i.e. signal intensity contribution of each fragment to the total signal, (AMS-mass fractions). Therefore only a qualitative comparison is performed in this figure, showing that the spectrum contains more fragments in the mass range m/z 100-200 at 50 min than at 150 min of reaction.

In the new version of the manuscript, we replaced “*normalized AMS-signal*” by “*AMS mass fraction*” in Figures 3 and 4, and we explained the term in the captions: “*The AMS-mass fraction is the signal intensity contribution of each fragment to the total signal.*”

- Calibration experiments of our set up were performed using aqueous solutions of three different compounds (NaCl, NH_4NO_3 , and succinic acid) at various concentrations covering those of the consumed MVK during its reaction (Table S1). In these calibration experiments, for each compound, the obtained numbers of particles increase with increasing solution concentrations, and the corresponding total particle mass increases linearly with the solution concentration. This result is used to evaluate the transmission efficiency of our set up. Assuming a similar behavior for the nebulized MVK-oligomers up to t_{max} (i.e. increasing oligomer concentrations with reaction time, assuming no major change in the oligomer composition), the calibration experiments are used to determine the SOA mass yields according to equations 2 and 3 of the new version of the manuscript. However, this protocol induces very large uncertainties (e.g. $Y_{\text{SOA}} = 70 (\pm 50)\%$ at 105 minutes of reaction in exp A). A different experimental protocol, that does not use the nebulizer, has been developed (i.e. preparative chromatography followed by TOC analysis, as described in sections 2.2.4 and 3.2.3) to determine the SOA mass yield, and confirm the obtained numbers with narrower uncertainties ($Y_{\text{SOA}} = 59 (\pm 5)\%$ at 90 minutes of reaction in exp A).

All these precisions have been added in supplementary information 1, it now reads:

“Calibration experiments of our set up were performed using aqueous solutions of three different compounds (NaCl, NH_4NO_3 , and succinic acid) at various concentrations covering those of the consumed MVK during its reaction (Table S1). In these calibration experiments, for each compound, the obtained numbers of particles increase with increasing solution concentrations, and the corresponding total particle mass (using the corresponding densities)

increases linearly with the solution concentration. This result was used to evaluate the transmission efficiency of our set up. Assuming a similar behavior for the nebulized MVK-oligomers up to t_{max} (i.e. increasing oligomer concentrations with reaction time, assuming no major change in the oligomer composition), the calibration experiments were used to determine the SOA mass yields according to equations 2 and 3. The differences obtained between the three calibration experiments may be due to the different physical properties of the particles (e.g. volatility, surface tension and hygroscopicity) linked to their chemical composition. Table S1 shows that the solutions of NaCl generated a significantly higher transmission efficiency than the solutions of NH_4NO_3 and succinic acid. It is likely that the properties of the SOA generated from the nebulized solutions of oxidized MVK were closer to that of NH_4NO_3 and succinic acid than NaCl. Finally, the transmission efficiency obtained for NH_4NO_3 solutions was used to calculate the SOA mass yields according to equations 2 and 3.”

Question 6.

Caption to Figure 8. I am not sure what the authors mean by the comparison to the data of Lee et al., 2001?

Answer:

The aim of the comparison was to highlight the similarity of the oxidation (aging) processes evidenced here with previous studies (Lee et al., 2011; Ng et al., 2010), despite differences in conditions. We have modified the text to make this point clearer, it now reads:

“In order to compare our work with the aging of organic aerosol in the atmosphere compiled by Ng et al. (2010), we used the AMS data, and in particular, the development of the two dominant fragments, m/z 44 (CO_2^+) and m/z 43 (mostly $C_2H_3O^+$), observed in our study. More precisely, we focused on the ratio of m/z 44 and m/z 43 to total organic aerosol, f_{44} and f_{43} , respectively. In Ng et al. (2010), low volatility oxygenated organic aerosol (LV-OOA) has higher f_{44} than semi-volatile oxygenated organic aerosol (SV-OOA) which in turn has higher f_{43} values. Despite the very different conditions, it is interesting to compare our aging data with those compiled from field studies and other aqueous phase experiments. Figure 8 compares our f_{44} versus f_{43} values to those provided in the compilation by Ng et al. (2010) as well as the

nebulization data by Lee et al., (2011a). It is clear from this figure that the SOA composition and its evolution highly depend on the initial MVK concentration.

References:

- Daumit, K. E., Carrasquillo, A. J., Hunter, J. F. and Kroll, J. H.: Laboratory studies of the aqueous-phase oxidation of polyols: submicron particles vs. bulk aqueous solution, *Atmospheric Chemistry and Physics*, 14(19), 10773–10784, doi:10.5194/acp-14-10773-2014, 2014.
- Hobby, K.: A novel method of isotope prediction applied to elemental composition analysis, 2005.
- Kameel, F. R., Hoffmann, M. R. and Colussi, A. J.: OH Radical-Initiated Chemistry of Isoprene in Aqueous Media. Atmospheric Implications, *The Journal of Physical Chemistry A*, 117(24), 5117–5123, doi:10.1021/jp4026267, 2013.
- Kameel, F. R., Riboni, F., Hoffmann, M. R., Enami, S. and Colussi, A. J.: Fenton Oxidation of Gaseous Isoprene on Aqueous Surfaces, *The Journal of Physical Chemistry C*, 140725063829009, doi:10.1021/jp505010e, 2014.
- Lee, A. K. Y., Herckes, P., Leaitch, W. R., Macdonald, A. M. and Abbatt, J. P. D.: Aqueous OH oxidation of ambient organic aerosol and cloud water organics: Formation of highly oxidized products: AQUEOUS OXIDATION OF AMBIENT ORGANICS, *Geophysical Research Letters*, 38(11), n/a–n/a, doi:10.1029/2011GL047439, 2011a.
- Lee, A. K. Y., Zhao, R., Gao, S. S. and Abbatt, J. P. D.: Aqueous-Phase OH Oxidation of Glyoxal: Application of a Novel Analytical Approach Employing Aerosol Mass Spectrometry and Complementary Off-Line Techniques, *The Journal of Physical Chemistry A*, 115(38), 10517–10526, doi:10.1021/jp204099g, 2011b.
- Ng, N. L., Canagaratna, M. R., Zhang, Q., Jimenez, J. L., Tian, J., Ulbrich, I. M., Kroll, J. H., Docherty, K. S., Chhabra, P. S., Bahreini, R., Murphy, S. M., Seinfeld, J. H., Hildebrandt, L., Donahue, N. M., DeCarlo, P. F., Lanz, V. A., Prévôt, A. S. H., Dinar, E., Rudich, Y. and Worsnop, D. R.: Organic aerosol components observed in Northern Hemispheric datasets from Aerosol Mass Spectrometry, *Atmospheric Chemistry and Physics*, 10(10), 4625–4641, doi:10.5194/acp-10-4625-2010, 2010.
- Renard, P., Reed Harris, A. E., Rapf, R. J., Ravier, S., Demelas, C., Coulomb, B., Quivet, E., Vaida, V. and Monod, A.: Aqueous Phase Oligomerization of Methyl Vinyl Ketone by Atmospheric Radical Reactions, *The Journal of Physical Chemistry C* [online] Available from: <http://pubs.acs.org/doi/abs/10.1021/jp5065598> (Accessed 23 October 2014), 2014.
- Renard, P., Siekmann, F., Gandolfo, A., Socorro, J., Salque, G., Ravier, S., Quivet, E., Clément, J.-L., Traikia, M., Delort, A.-M., Voisin, D., Vuitton, V., Thissen, R. and Monod, A.: Radical mechanisms of methyl vinyl ketone oligomerization through aqueous phase OH-oxidation: on the paradoxical role of dissolved molecular oxygen, *Atmospheric Chemistry and Physics*, 13(13), 6473–6491, doi:10.5194/acp-13-6473-2013, 2013.
- Tan, Y., Lim, Y. B., Altieri, K. E., Seitzinger, S. P. and Turpin, B. J.: Mechanisms leading to oligomers and SOA through aqueous photooxidation: insights from OH radical oxidation of acetic acid and methylglyoxal, *Atmospheric Chemistry and Physics*, 12(2), 801–813, doi:10.5194/acp-12-801-2012, 2012.

Zhao, R., Lee, A. K. Y. and Abbatt, J. P. D.: Investigation of Aqueous-Phase Photooxidation of Glyoxal and Methylglyoxal by Aerosol Chemical Ionization Mass Spectrometry: Observation of Hydroxyhydroperoxide Formation, *The Journal of Physical Chemistry A*, 116(24), 6253–6263, doi:10.1021/jp211528d, 2012.

Referee 4

Interactive comment on “Aqueous phase oligomerization of methyl vinyl ketone through photooxidation – Part 1: Aging processes of oligomers” by P. Renard et al.

RC C4782: Anonymous Referee #4, 13 Jul 2014

The authors appreciate many important comments raised by Reviewer 4 which have been considered in the new version of the manuscript. The authors' answers to the questions/comments of Reviewer 4 are presented below.

General:

Comment 1:

The $[\text{MVK}]_0 / [\text{H}_2\text{O}_2]_0$ ratio is always 20. Recently there has been evidence in the literature that oxidant-limited conditions influence the amount of SOA formed in aqueous phase experiments, both in laboratory (Nguyen et al., ACP, 2014) and modeling (Ervens et al, JGR, 2014) work. Can the authors describe their understanding in this context, with specific reference to how conditions here are not oxidant limited?

Answer :

Under our experimental conditions, the decay of MVK concentrations down to 0 shows that our conditions are not oxidant limited. Furthermore, these conditions allow for steady state concentrations of OH radicals of $\sim 10^{-14}$ M (see the determinations in Supplementary information 2 of the new version of the manuscript), which fall in the range of the estimated values for cloud and fog droplets (Herrmann et al., 2010; Ervens and Volkamer, 2010 and Arakaki et al., 2013).

Comment 2:

Some of the language is awkward. For example, AMS signal climax should be changed to something along the lines of “maximum AMS signal intensity”.

Answer : the text has been changed according to this comment, it now reads: “At 50 min the maximum of oligomerization is reached (Figure 2c).”

Comment 3:

There are a few mis-matched singular/plural noun/verb combinations that should be corrected.

Answer :

Done.

Comment 4:

Detailed comments: p.15256, “: : : in particular, in regions with high relative humidity (Carlton and Turpin, 2013)”. Please add “and hygroscopic aerosol” after relative humidity.

Answer :

Done.

Comment 5:

Is it possible to add uncertainty bars to Figures 3, 5 and 10 (like for Figure 6)?

Answer :

Done, uncertainty bars can not appear in figure 5.

References:

- Arakaki, T., Anastasio, C., Kuroki, Y., Nakajima, H., Okada, K., Kotani, Y., Handa, D., Azechi, S., Kimura, T., Tsuchi, A. and Miyagi, Y.: A General Scavenging Rate Constant for Reaction of Hydroxyl Radical with Organic Carbon in Atmospheric Waters, *Environmental Science & Technology*, 130718140737000, doi:10.1021/es401927b, 2013.
- Carlton, A. G. and Turpin, B. J.: Particle partitioning potential of organic compounds is highest in the Eastern US and driven by anthropogenic water, *Atmospheric Chemistry and Physics*, 13(20), 10203–10214, doi:10.5194/acp-13-10203-2013, 2013.
- Ervens, B., Sorooshian, A., Lim, Y. B. and Turpin, B. J.: Key parameters controlling OH-initiated formation of secondary organic aerosol in the aqueous phase (aqSOA): KEY PARAMETERS OF AQSOA FORMATION, *Journal of Geophysical Research: Atmospheres*, 119(7), 3997–4016, doi:10.1002/2013JD021021, 2014.
- Ervens, B. and Volkamer, R.: Glyoxal processing by aerosol multiphase chemistry: towards a kinetic modeling framework of secondary organic aerosol formation in aqueous particles, *Atmospheric Chemistry and Physics*, 10(17), 8219–8244, doi:10.5194/acp-10-8219-2010, 2010.
- Herrmann, H., Hoffmann, D., Schaefer, T., Brüner, P. and Tilgner, A.: Tropospheric Aqueous-Phase Free-Radical Chemistry: Radical Sources, Spectra, Reaction Kinetics and Prediction Tools, *ChemPhysChem*, 11(18), 3796–3822, doi:10.1002/cphc.201000533, 2010.
- Nguyen, T. K. V., Petters, M. D., Suda, S. R. and Carlton, A. G.: Trends in particle phase liquid water during the Southern Oxidant and Aerosol Study, *Atmospheric Chemistry and Physics Discussions*, 14(6), 7469–7516, doi:10.5194/acpd-14-7469-2014, 2014.

Aqueous phase oligomerization of methyl vinyl ketone through photooxidation

Part 1: Aging processes of oligomers

Pascal Renard¹, Frank Siekmann¹, Guillaume Salque², Carine Demelas¹, Bruno Coulomb¹, Laurent Vassalo¹, Sylvain Ravier¹, Brice Temime-Roussel¹, Didier Voisin², Anne Monod¹

¹ Aix-Marseille Université, CNRS, LCE FRE 3416, 13331, Marseille, France

² Université Joseph Fourier, Grenoble 1 / CNRS-INSU, Laboratoire de Glaciologie et Géophysique de l'Environnement, 54 rue Molière, 38402 Saint-Martin-d'Hères, France

Abstract

It has recently been established that unsaturated water soluble organic compounds (UWSOC) might efficiently form oligomers in polluted fogs and wet aerosol particles, even for weakly soluble ones like methyl vinyl ketone (MVK). The atmospheric relevance of these processes is explored by means of multiphase process model studies (in a companion paper). In the present study, we investigate the aging of these aqueous phase MVK-oligomers formed via [•]OH-oxidation, as well as their ability to form secondary organic aerosol (SOA) upon water evaporation. The comparison between aqueous phase composition and aerosol composition after nebulization of the corresponding solutions shows similar trends for oligomer formation and aging. The measurements reveal that oligomer aging leads to the formation of organic diacids. Quantification of the SOA mass formed after nebulization is performed, and the obtained SOA mass yields seem to depend on the spectral irradiance of the light used to initiate the photochemistry. Investigating a large range of initial MVK concentrations (0.2 – 20 mM), the results show that its [•]OH-oxidation undergoes competition between functionalization and oligomerization that is dependent on the precursor concentration. At high initial MVK concentrations (≥ 2 mM), oligomerization prevails over functionalization, while at lower initial concentrations, oligomerization is not the major process, and functionalization dominates, resulting in small carbonyls, dicarbonyls and monoacids. The atmospheric implications of these processes are discussed.

1 ~~Secondary organic aerosol (SOA) represents a substantial part of organic aerosol, which~~
2 ~~affects climate and human health. It is now accepted that one of the important pathways of~~
3 ~~SOA formation occurs via aqueous phase chemistry in the atmosphere. Recently, we have~~
4 ~~shown in a previous study (Renard et al., 2013) the mechanism of oligomerization of MVK~~
5 ~~(methyl vinyl ketone), and suggested that unsaturated water soluble organic compounds~~
6 ~~(UWSOC) might efficiently form SOA in wet aerosol particles, even for weakly soluble ones~~
7 ~~like MVK. The atmospheric relevance of these processes is explored by means of process~~
8 ~~model studies (in a companion paper). In the present study we investigate the aging of these~~
9 ~~aqueous phase MVK oligomers (Part 1).~~

10 ~~We compared aqueous phase composition and SOA composition after nebulization, mainly by~~
11 ~~means of UPLC-ESI-MS and AMS, respectively. Both instruments match and show similar~~
12 ~~trend of oligomer formation and aging. The SMPS analysis performed on the nebulized~~
13 ~~solutions allow to quantify these SOA and to measure their mass yields.~~

14 ~~We have highlighted in the current study that MVK \bullet OH oxidation undergoes kinetic~~
15 ~~competition between functionalization and oligomerization. The SOA composition and its~~
16 ~~evolution highly depend on the precursor initial concentration. We determined the threshold~~
17 ~~of MVK concentration, i.e. 2 mM, from which oligomerization prevails over~~
18 ~~functionalization. Hence, at these concentrations, \bullet OH oxidation of MVK forms oligomers~~
19 ~~that are SV OOA, with low O/C and high f₄₃. Oligomers are then fragmented, via~~
20 ~~unidentified intermediates that have the properties of LV OOA which then end into succinic,~~
21 ~~malonic and oxalic diacids. For lower initial MVK concentrations, the oligomerization is not~~
22 ~~the major process, and functionalization dominates, resulting in small carbonyls, dicarbonyls~~
23 ~~and mainly monoacids.~~

24 ~~The aging of these oligomers could be an explanation for the presence of a part of the diacids~~
25 ~~observed in aerosol.~~

26 **1. Introduction**

27 Organic aerosol plays an important role in many atmospheric processes and has an important
28 impact on climate and human health. Globally, about 20 % of the organic aerosol mass is
29 emitted directly (Kanakidou et al., 2005; Spracklen et al., 2011), which conversely indicates
30 the relevance of aerosol formed secondarily by transformation of organic gas phase species,
31 *i.e.* secondary organic aerosol (SOA). The most commonly studied mechanism of SOA
32 formation is the oxidation of volatile organic compounds (VOCs), which can lead to the

1 formation of less volatile species that subsequently partition into the condensed phase
2 (Donahue et al., 2011; Kanakidou et al., 2005; Kroll and Seinfeld, 2008; Hallquist et al.,
3 2009). Nevertheless, the oxidation of VOCs also results in more water soluble products that
4 readily partition into the aqueous phase (Blando and Turpin, 2000; Ervens et al., 2011;
5 Epstein et al., 2013). Due to further reactivity in the liquid phase, higher molecular weight and
6 less volatile compounds can be formed, which can remain at least in part in the condensed
7 phase upon water evaporation, thus leading to additional secondary organic aerosol formation
8 through aqueous phase reactions (aqSOA) (El Haddad et al., 2009; Carlton et al., 2009;
9 Ervens et al. 2011; Ortiz-Montalvo et al., 2012). In particular, Lee et al. (2012) observed a
10 significant enhancement of organic mass during the initial stage of oxidation of cloud water
11 organics, that they explained by functionalizing dissolved volatile organics *via* hydroxyl
12 radical ($\cdot\text{OH}$) oxidation. Aqueous phase processes can be very different from those in the gas
13 phase, thus leading to aqSOA with likely very different physical and chemical properties
14 (Ervens et al. 2011; Ortiz-Montalvo et al., 2012). These differences can explain that the
15 oxidation state of SOA formed during dry smog chamber experiments is significantly lower
16 than that of ambient SOA (Kroll and Seinfeld, 2008; Aiken et al., 2008; De Carlo et al., 2008;
17 Ng et al., 2010; Lee et al., 2012).

18 Volkamer et al. (2007) suggested that chemical processes in the aqueous phase of hygroscopic
19 particles (wet aerosol) can efficiently contribute to aqSOA mass. Besides, wet aerosol
20 provides higher precursor concentrations than in cloud and fog water droplets and reside in
21 the atmosphere over hours or days (Ervens et al., 2011), suggesting a significant role for
22 aqSOA formation in wet aerosol, in particular, in regions with high relative humidity (Carlton
23 and Turpin, 2013) and hygroscopic aerosol. Isoprene has the largest global atmospheric
24 emissions (estimated at $\sim 600 \text{ Tg yr}^{-1}$ Guenther et al., 2006) of all non-methane VOCs. Its key
25 oxidation products, *i.e.* methacrolein (MACR) and hydroperoxides (Kroll et al., 2006) are
26 known to contribute directly to the formation of SOA in the atmosphere. Methyl vinyl ketone
27 (MVK) is the other main gas-phase oxidation products of isoprene (yielding from 32 to 44 %,
28 Lee et al., 2005, Kroll et al., 2006). Unlike MACR, MVK does not lead to the formation of
29 SOA during its gas phase photooxidation (Kroll et al. 2006; Surratt et al 2006), likely because
30 of the lack of an aldehydic hydrogen which precludes the formation of acidic products such as
31 2,3-dihydroxymethacrylic acid (*i.e.* 2-methylglyceric acid: 2-MG) for further particle-phase
32 esterification reactions (Surratt et al., 2006). However, these results were obtained in smog

1 chamber experiments performed under dry conditions where aqueous phase processes were
2 excluded.

3 The photooxidation of carbonyl compounds ~~linked to isoprene reactivity~~ has been studied in
4 the aqueous phase, and their ability to form oligomers and potentially aqSOA was shown
5 (Altieri et al., 2006 and 2008; Carlton et al., 2006 and 2007; Perri et al., 2009; El Haddad et
6 al., 2009; Tan et al., 2009, 2010 and 2012; Zhang et al., 2010; Zhao et al., 2012; Liu et al.,
7 2012; Ortiz-Montalvo et al., 2012; Lim et al., 2013; Renard et al., 2013; Kameel et al., 2013;
8 Kameel et al., 2014; Daumit et al., 2014). In particular, Renard et al. (2013) showed that [•]OH
9 oxidation of MVK in the aqueous phase proceeds via a radical mechanism leading to
10 oligomers which molecular masses increase (up to m/z 1200) with the precursor initial
11 concentration from 2 to 20 mM. At lower precursor initial concentrations (e.g. 0.2 mM of
12 MVK), Renard et al. (2013) observed lower weight molecular compounds (up to m/z 300),
13 and Zhang et al., (2010) observed the formation of small oxidized compounds (such as acetic,
14 formic, pyruvic acids, methylglyoxal, formaldehyde), thus suggesting a competition between
15 functionalization and oligomerization at these low initial concentrationsIn particular, Renard
16 et al. (2013) showed that [•]OH oxidation of MVK (> 2mM) in the aqueous phase proceeds via
17 a radical mechanism leading to oligomers which molecular masses increase with the precursor
18 initial concentration. In contrast, at lower precursor initial concentrations, Zhang et al. (2010)
19 mainly observed low weight molecular compounds, such as low volatility organic acid,
20 suggesting functionalization might dominate over oligomerization.

21 Liu et al. (2012) showed the ability of the generated oligomers to form SOA after water
22 evaporation. It is thus likely that the atmospheric impact of MVK reactivity, and especially its
23 ability to form SOA, is very different under dry and humid conditions.

24 The aim of the present study is to investigate the aging of the oligomers formed through
25 aqueous phase photooxidation of MVK. We determine the SOA chemical composition during
26 the formation and aging of the aqueous phase oligomers and we revisit the corresponding
27 SOA mass yields. A large range of initial precursor concentrations (from 0.2 to 20 mM); is
28 investigated in order to study the competition between functionalization and oligomerization.

29
30 ~~Considering MVK as a proxy for unsaturated water soluble organic compounds (UWSOC),~~
31 ~~these concentrations are atmospherically relevant, in particular in wet aerosols (Ervens et al.,~~
32 ~~2011; Renard et al., 2013). In a companion paper (Ervens et al., in preparation), we will~~
33 ~~discuss the explicit chemical mechanism of oligomer formation (as described in Renard et al.,~~

1 | ~~2013) and loss and explore the atmospheric relevance of these processes by means of process~~
2 | ~~model studies.~~

3 | **2. Experimental**

4 | A photoreactor was used to simulate the aqueous phase photooxidation of MVK. $\cdot\text{OH}$
5 | radicals were generated from H_2O_2 photolysis (Table 1). The liquid phase was analyzed using
6 | ~~a variety of analyzers for qualitative and quantitative characterization of the solution (detailed~~
7 | ~~in section 2.2). ultra-performance liquid chromatography mass spectrometry (UPLC-ESI-~~
8 | ~~MS), ionic chromatography mass spectrometry (IC-ESI-MS), a total organic carbon (TOC)~~
9 | ~~analyzer and Ultra High Performance Liquid Chromatography UV (UHPLC-UV).~~

10 | For aerosol generation, aliquots of the solution were sampled from the photoreactor at specific
11 | reaction times, then nebulized and dried prior to aerosol characterization using a scanning
12 | mobility particle sizer (SMPS) and a high resolution time-of-flight aerosol mass spectrometer
13 | (AMS) (Figure 1). Each experiment (aqueous phase photooxidation and aerosol generation)
14 | was repeated at least once.

15 | **2.1 Photoreactor**

16 | ~~The photoreactor set-up used was based on the one described by Renard et al., (2013). It was~~
17 | ~~a 450 cm³ Pyrex thermostated photoreactor, equipped with a 1000 Watt Xenon arc lamp~~
18 | ~~(LOT-Oriel, LSH 601) and a glass filter (ASTM 490 AM 0). The resulting spectral irradiance~~
19 | ~~into the reactor is compared to that of the sun at sea level for a 48.3° zenith angle~~ Figure S1.

20 | All experiments were performed at 25°C and started with irradiation of UHQ water (18.2 MΩ
21 | cm, Millipore), then H_2O_2 (Acros, 30 %, non-stabilized) was introduced, and after 10 min of
22 | H_2O_2 photolysis, MVK (Sigma Aldrich, 99 %) was introduced at time 0.

23 | Tan et al. (2010) and Renard et al. (2013) have shown the important impact of initial
24 | concentrations on oligomer formation. The experiments were thus carried out with various
25 | MVK initial concentrations (Table 1), *i.e.*, 0.2, 0.5, 2, 5 and 20 mM (corresponding to 9.6 to
26 | 960 mgC L⁻¹). Considering MVK as a proxy for UWSOC, this concentration range is
27 | comprised in the range of the estimated total UWSOC concentrations from fog droplets to wet
28 | aerosol (Renard et al., 2013).

29 | The 50 cm³ gas phase head space of the photoreactor was opened to ambient air for a few
30 | seconds during each sampling. We verified in control experiments that this procedure induced
31 | insignificant losses of MVK from the solution.

1 The initial H₂O₂ concentrations were chosen in order to obtain a ratio ($\frac{[H_2O_2]_0}{[MVK]_0} = 20$), in order
2 to favor ·OH reaction with MVK rather than with H₂O₂ by more than 90 %. Under these
3 conditions, ·OH concentrations were estimated in the range (2 - 6) × 10⁻¹⁴ M (*organic aerosol*
4 (*LV-OOA*) elementary information SI2), which falls in the range of the estimated values for
5 ·OH concentrations in cloud and fog droplets (Herrmann et al., 2010; Ervens and Volkamer,
6 2010 and Arakaki et al., 2013).

7 **2.2 Aqueous phase characterization**

8 Aliquots of the solution sampled from the photoreactor were analyzed for qualitative structure
9 elucidation of the oligomers using ultra-performance liquid chromatography mass
10 spectrometry (UPLC-ESI-MS); and for quantitative studies of the concentrations of i) MVK
11 and H₂O₂ by liquid chromatography coupled to UV detection (UHPLC-UV), iii) carboxylic
12 acids by ion chromatography-mass spectrometry (IC-ESI-MS), and iv) oligomers using
13 preparative liquid chromatography associated to total organic carbon (TOC) analyses.

14 *2.2.1 UPLC-ESI-MS analyses*

15 Aliquots of the solution sampled from the photoreactor were analyzed for organic species
16 using an ultra-high performance liquid chromatographic system coupled to a time of flight
17 mass spectrometer equipped with an electrospray source and an ion mobility cell (Synapt-G2
18 HDMS, Waters). The mass spectrometer was used in its resolution mode (V-mode), up to
19 18,000 FWHM (Full width at half maximum) at m/z 400. The mass accuracy was < 5 ppm,
20 and allowed for the determination of elemental composition of organic species (Renard et al.,
21 2013 and Renard et al., 2014), using the I-FIT software. The I-FIT isotope predictive filtering
22 is a strategy to reduce the number of proposed elemental compositions using algorithms to
23 estimate the number of carbon, oxygen (or sulfur) atoms in an unknown molecule based on
24 the mass of the molecular ion and the relative intensity of the 1st and 2nd isotopes (Hobby,
25 2005).

26 All parameters used are detailed in Renard et al., (2013). Briefly, the chromatographic
27 separations were carried out on an UPLC column (Waters, HSS T3 C18, 2.1 * 100 mm – 1.8
28 μm) at 40°C. The mobile phases consisted in (A) 0.1 % formic acid (Biosolve, 99 %) in water
29 and (B) acetonitrile (Biosolve, ULC/MS). The gradient elution was performed at a flow rate
30 of 600 μL min⁻¹ using 5 to 95 % of B within 7 min and held at 95 % of B for 1.5 min. The
31 sample injection volume was 10 μL.

1 During each chromatographic run, leucine enkephalin (Waters, 2 ng μL^{-1} , $\text{C}_{28}\text{H}_{37}\text{N}_5\text{O}_7$) was
2 used for lock-mass correction to obtain accurate masses for each organic component eluting
3 from the column. Optimum ESI conditions were found using a 0.5 kV capillary voltage, 40 V
4 sample cone voltage, 450°C desolvation temperature, 120°C source temperature, 20 L h^{-1}
5 cone gas flow rate and 800 L h^{-1} desolvation gas flow rate.

6 All products were detected as their protonated molecules ($[\text{M} + \text{H}]^+$) or sodium adducts ($[\text{M} +$
7 $\text{Na}]^+$) in the positive mode, and their deprotonated molecules ($[\text{M} - \text{H}]^-$) in the negative
8 mode. Data were collected from m/z 50 to 1800 in both ionization modes.

9 2.2.2 UHPLC-UV analyses

10 An ultra-high performance liquid chromatographic (UHPLC) system (ThermoScientific,
11 Accela 600 auto sampler and Accela 600 pump) coupled to a diode array detector
12 (ThermoScientific, Accela 600 PDA detector) was used to monitor the concentrations of
13 MVK and H_2O_2 sampled from the photoreactor. The chromatographic separation was
14 performed using a column (ThermoScientific, Hypersil GOLD, 100 x 2.1 mm - 1.9 μm
15 ThermoScientific) at 40°C and a flow rate of 300 $\mu\text{L min}^{-1}$. The mobile phase was
16 water/acetonitrile (98:2) (v/v) and the injection volume was set to 2 μL . The spectra were
17 recorded from 200 to 360 nm.

18 Under these conditions, H_2O_2 has a retention time of 0.5 minutes and is chromatographically
19 separated from MVK which has a retention time of 1.8 minutes. The UHPLC-UV spectrum of
20 aqueous H_2O_2 exponentially increases with decreasing wavelength, it becomes intense below
21 300 nm and peaks below the detection limit of the instrument ($< 190 \text{ nm}$). Aqueous solutions
22 of MVK show an intense absorption band (K-band; $\pi \rightarrow \pi^*$ transition) that peaks at 211 nm
23 and a weak absorption band (R-band; $n \rightarrow \pi^*$ transition) that peaks at 308 nm. The absorption
24 intensity chromatograms were monitored at 270, 229 nm and 211 nm and the peak areas
25 were found to be directly proportional to both the H_2O_2 and the MVK concentrations in the
26 range of the studied concentrations: at 211 nm for low MVK concentrations ($[\text{MVK}] \leq 2$
27 mM), at 229 nm for $[\text{H}_2\text{O}_2] \leq 400 \text{ mM}$ and $2 < [\text{MVK}] \leq 20 \text{ mM}$, and at 270 nm for higher
28 concentrations of H_2O_2 (up to 400 mM).

29 2.2.3 IC-ESI-MS analyses

30 Quantification of organic acids in the solutions was performed with an ion chromatography
31 system (Dionex ICS3000) driven by Chromeleon[®] software (6.80 version), composed of a
32 gradient pump (Dionex SP-5), an autosampler (Dionex AS40), a conductivity detector

1 (Dionex, CD25) and coupled to a quadrupole mass spectrometer (Thermo Scientific Surveyor
2 MSQ) operated in the negative electrospray ionization (ESI) mode, with nitrogen gas (gas
3 flow: 6 L h⁻¹, 40 psi, temperature 500°C; Capillary voltage 3,5 kV; Sample cone voltage 75
4 V). A electrolytic suppressor (Dionex, 4 mm ASRS 300) operated in external water mode (7
5 mL min⁻¹) was placed before the conductivity cell. An additional peristaltic pump was used
6 during measurements to wash the entrance cone of the mass spectrometer with water at a flow
7 rate of 0.4 mL min⁻¹. The chromatographic separations were carried out on a column (Dionex,
8 IonPac AS11-HC, 4 x 250 mm) coupled to a guard column (Dionex, AG11-HC, 4 x 50 mm).
9 A 25 µL sample was injected automatically using a 25 µL loop injection valve. The analysis
10 was performed at 35°C, with a flow rate set at 0.8 mL min⁻¹. Eluent A (Ultra High Quality
11 water) and eluent B (100 mM NaOH) were flushed with purified helium gas for 30 min and
12 kept under nitrogen atmosphere during the procedure. Separation was carried out using the
13 following gradient (min, B %): 0, 1 %; 12, 5 %; 30, 19 %; 40, 40 %, 50, 1 %. The analytes
14 were monitored using the selected ion-monitoring (SIM) mode, and signal areas (counts min⁻¹
15 ¹) of each peak were used for quantification.

16 2.2.4 TOC analyses

17 TOC measurements were coupled to preparative liquid chromatography to
18 separate the oligomers from the small and/or volatile reactants and reaction products in the
19 liquid samples, in order to measure the SOA oligomer mass yields in experiment A (see
20 section 3.2.3). A total organic carbon / total nitrogen (TOC/TN) analyzer (Analytik Jena,
21 N/C2100S) with the non-purgeable organic carbon (NPOC) method was used to quantify the
22 produced oligomers in our liquid samples.

23 The NPOC method consists in pre-purging samples with oxygen and pre-acidifying (at pH=2
24 with HCl) to remove the inorganic carbon and purgeable organic carbon. TOC is measured by
25 injecting the sample into a heated combustion tube (800°C) with an oxidation catalyst. The
26 CO₂ produced is measured by a non-dispersive infrared (NDIR) gas analyzer. TN is measured
27 in parallel using chemiluminescence detection (CLD).

28 2.3 Particle generation and characterization

29 For aerosol generation, 35 mL of the solution was sampled at specific reaction times (Table
30 1), and nebulized using an atomizer (TSI, 3079) with a flow rate of 3.5 L min⁻¹ (Figure 1).
31 The generated droplet flow was led through a silica gel diffusion dryer and diluted with
32 filtered ambient air (at 5 L min⁻¹, using a HEPA capsule filter). A small fraction of the sample

1 ($\approx 0.4 \text{ L min}^{-1}$) was passed through a Nafion dryer (Permapure, MD-110), before entering a
2 small 100 mL glass mixing chamber and the on-line analytical devices. The obtained relative
3 humidity was constant during all experiments at ca. 15 % measured at the entrance of the
4 AMS (Figure 1). The nebulization time for each sample was 30 min and, to ensure constant
5 and reproducible aerosol generation, only the last 15 min of nebulization were employed for
6 data analysis. To avoid memory effects, before each nebulization experiment, the system was
7 flushed by nebulizing UHQ water for 30 min.

8 The number size distribution was measured using a scanning mobility particle sizer (SMPS),
9 (Grimm, SMPS+C) consisting of a differential mobility analyzer (L-DMA) with a
10 condensation particle counter (Grimm, CPC, 5.403). The analyzed particle size ranged from
11 11 to 1083 nm (scanned within 6 min and 43 s).

12 A high resolution time-of-flight aerosol mass spectrometer was used to measure the bulk
13 chemical composition of the non-refractory submicron particulate matter (De Carlo et al.
14 2006; Canagaratna et al., 2007). The instrument was used under standard conditions
15 (vaporizer at 600°C and electron ionization at 70 eV), in the high sensitivity V-mode (up to
16 2000 at m/z 200). Each measurement point was averaged for 2 min and 40 s (MS- and PToF-
17 cycle, 40 s each, 2 cycles per run). Mass spectra of filtered air (using a HEPA capsule filter)
18 were taken prior each series of nebulizing experiments in order to adjust the m/z 44 entry of
19 the fragmentation table due to gas phase CO₂.

20 The standard fragmentation table with the corrected air fragment column for our carrier gas
21 and the default values of relative ionization efficiency were used in the AMS data analysis
22 (Squirrel 1.51H and the software PIKA 1.10H).

23 **3. Results**

24 We investigated MVK-[•]OH oxidation in the aqueous phase and subsequent SOA formation
25 upon water evaporation, by nebulizing the liquid solution. During this process, oligomer
26 formation and aging was monitored, and a qualitative and a quantitative study of the SOA
27 formed after nebulization was performed. For these investigations, a large range of initial
28 MVK concentrations (0.2 – 20 mM) was explored.

29 in aqueous phase, using UPLC-ESI-MS; and in parallel, gathers qualitative (section 3.1) and
30 quantitative (section 3.2) study of oligomers after nebulization, by means of HR-ToF-AMS
31 and SMPS, respectively.

1 3.1 Evidence for oligomer formation and aging

2 During MVK- \cdot OH oxidation, the aqueous phase composition was monitored and compared to
3 the composition of the corresponding nebulized solutions.

4 3.1.1 Aqueous phase analyses

5 For each experiment, the solution was directly monitored using UPLC-ESI-MS and UHPLC-
6 UV for reaction times up to 150 min (Table 1). This time was higher than the complete
7 consumption of MVK in order to study the formation of oligomers and their aging processes,
8 as illustrated in Figure 2.

9 During experiment B (*i.e.* $[\text{MVK}]_0 = 5\text{mM}$), after 5 minutes of reaction, no significant
10 formation of high molecular weight compounds (HMWC) was observed (Figure 2b), whereas
11 after 10 minutes of reaction, mass spectra show that oligomer systems were formed on the
12 whole range of the investigated m/z (50-1200), with a regular pattern of 70.042 amu, which
13 corresponds to the exact mass of MVK. At 50 minutes of reaction, the maximum of
14 oligomerization ~~elimax is~~ was reached (Figure 2c). At this time, we observed several series of
15 MVK-oligomers, corresponding to several initiator radicals identified by Renard et al. (2013)
16 under the same conditions. As an example, the molecular structure of the most intense series
17 is given in Figure 2c and is highlighted in red in the mass spectrum. At that time, 90 % of
18 MVK was consumed. Finally, the intensities of all the oligomer series decreased
19 simultaneously for all masses with no change in the oligomer pattern up to 90 minutes. From
20 this reaction time, the mass spectra show a collapse of the regular pattern in both negative
21 (Figure 2d, 150 min) and positive modes, certainly corresponding to a drastic aging process in
22 which oligomers formed smaller molecules. This hypothesis is confirmed by a more global
23 approach, using the SMPS and the AMS analysis of the SOA formed after nebulization of the
24 solutions.

25 3.1.2 Aerosol composition of SOA generated after nebulization of the solutions

26 Under similar conditions, we verified in a previous study (Liu et al., 2012) that nebulization
27 of the reacted solutions and subsequent aerosol particle drying processes induced negligible
28 chemical transformations of the oligomers compared to the aqueous phase composition. It was
29 thus meaningful to compare the compositions of aqueous phase and SOA after nebulization.

30 The AMS mass spectra (Figure 3) show two dominant fragments, at m/z 43 and m/z 44
31 (~~thought to be predominantly corresponding to $\text{C}_2\text{H}_3\text{O}^+$ and CO_2^+ for ambient OOA~~
32 ~~(oxygenated organic aerosol), respectively [Ng et al., 2010] fragments~~). The time profiles of

1 the AMS total organic mass and both fragments clearly show (Figure 3) the same three-step
2 kinetic behavior as the one described above in section 3.1.1 for the corresponding solutions
3 (Figure 2). Until 10 min of reaction, the intensity of the AMS total mass remains low (Figure
4 3a) and the mass spectrum at 5 min (Figure 3b) is not significantly different from the one
5 obtained by nebulizing an aqueous solution containing the reactants before reaction, with m/z
6 fragments lower than 100. Then, the total mass increases to reach a maximum at 50 min
7 (Figure 3c), an order of magnitude higher than at 5 min. The mass spectrum is dominated by
8 the m/z 43 fragment (Figure 3c). This observation is likely due to fragmentation (by electronic
9 impact of the AMS, Ng et al., 2010) of oligomers containing repetitive carbonyl functions
10 such as those identified in the aqueous phase (see the example of the molecular structure in
11 Figure 2c, and in Renard et al., 2013). Finally, the intensity of both the total organic mass and
12 that of m/z 43 fragment decrease, the one of m/z 44 increases, and they both dominate the
13 AMS mass spectrum with the same intensity at the end of our investigation (150 min, Figure
14 3d).

15 Furthermore, comparing the AMS mass spectra between 50 and 150 min at higher masses
16 (m/z 100 – 200) (Figure 4), it is clear that at 50 min of reaction, the mass spectrum contains
17 more fragments in this range, than at 150 min. It is thus likely that the oligomers are being
18 significantly photooxidized through a fragmentation mechanism that forms smaller acidic
19 compounds (as observed by [Aljawhary et al. \(2013\) for different precursors](#)), and it confirms
20 the oligomer aging process suggested in Figure 2. After 50 min, oligomer fragmentation
21 prevails over oligomer formation.

~~22 [These kinetics were obtained by means of a xenon lamp \(1000 W\). The lamp, with an](#)
23 [irradiance spectrum comparable to that of the sun but approximately twice as intense, halves](#)
24 [the time required to reach the maximum oligomers. The lifetime of aerosols being several](#)
25 [days \(Ervens et al., 2010\), oligomerization remains atmospherically relevant.](#)~~

~~26 [For the quantitative study \(section 3.2\), we used the data provided by the SMPS analysis.](#)
27 [Note that the overall collection efficiencies \(CE\) of the AMS in our experiments varied from](#)
28 [0.07 to 0.21 \(related to the SMPS signal\). These low CE values \(compared to chamber](#)
29 [studies or ambient aerosols\) mainly can be due to particle bounce at the vaporizer surface](#)
30 [before volatilization and to the shape and size-dependent transmission of the aerodynamic](#)
31 [lens. As a result, the studied compounds did not volatilize sufficiently fast at standard AMS](#)
32 [vaporizer temperatures to be correctly fully detected \(Liu et al., 2007; Docherty et al., 2013;](#)
33 [Miyakawa et al., 2013\).](#)~~

1 In addition to these effects, it is possible that our low CE values (compared to chamber studies
2 or ambient aerosols) were also due to the particle size range (50 nm - 150 nm mass
3 distribution), as the lowest part of this size range corresponds to the region where the AMS
4 transmission curve varies greatly (Liu et al., 2007). This effect is confirmed by the fact that
5 our lowest values for CE (0.07) were obtained for the lowest MVK initial concentrations (0.2
6 - 2 mM) where the smallest particles were formed (50 nm mass distribution).

7 **3.2 Quantitative study of SOA**

8 The oligomer formation, mass yields and aging were observed by the quantitative analyses
9 performed with the SMPS ~~on~~ measurements of the nebulized solutions.

10 *3.2.1 SOA mass*

11 For experiment B, Figure 5a shows a continuously increasing number size distribution with
12 reaction time from 5 to 150 min, with an increasing mode size during the two first kinetic
13 steps (up to 50 min), and a decreasing mode size during the third one, which corresponds to
14 oligomer aging. In order to determine the particle mass concentrations, we used the method
15 described by Kuwata et al. (2012) (eq. 1) to determine the density (ρ_{org}) of the SOA generated
16 in our system at each reaction time t ,

$$18 \quad \rho_{org, t} (\text{g cm}^{-3}) = \frac{12+1 \times (\text{H/C})_t + 16 \times (\text{O/C})_t}{7+5 \times (\text{H/C})_t + 4.15 \times (\text{O/C})_t} \quad (\text{eq. 1})$$

19
20 where $(\text{O/C})_t$ and $(\text{H/C})_t$ are elemental ratios at reaction time t , as determined by the AMS
21 analysis of the SOA formed in our system. These ratios extend to the same ranges as those
22 used by Kuwata et al. (2012), and the resulting particle densities are reported in Table 2 and
23 Table 3. In particular, Table 2 shows a substantial change in the H/C (decrease) and O/C
24 (increase) after 50 min of reaction (t_{max} , for which the maximum SOA mass is reached) for
25 experiment B, denoting the oligomer aging and inducing an increase of the aerosol density.

26 Using these particle densities, the total mass concentrations were determined, and the time
27 evolution of the resulting distribution particle mass concentrations is shown in Figure 5b for
28 experiment B. The blank signal was determined prior to each individual experiment by
29 nebulizing pure water samples and was subtracted in the results for the mass calculation. At
30 the initial reaction time (0 min), the particle size distribution was determined by nebulizing an
31 aqueous mixture of the reactants (using experiment B concentrations), it showed a mass

1 concentration ($11.0 \pm 1.4 \mu\text{g m}^{-3}$) not statistically different from the one obtained by
2 nebulizing pure water (assuming a density of 1.1 g cm^{-3}). This confirms that the reactants are
3 too volatile to form substantial amounts of organic aerosol by nebulization of the solution
4 prior to reaction.

5 Confirming the UPLC-ESI-MS aqueous phase analyses and the AMS results, a three-step
6 kinetic behavior is also observed on the SMPS total mass concentrations (Figure 5b and
7 Figure 6). A slow increase is observed during the first step (0 – 10 min). Then oligomerization
8 takes place corresponding to a fast increase of the SMPS mass, until 50 min. Finally, after this
9 ~~elimax~~maximum of oligomerization, a significant decrease of the SMPS mass is observed.
10 This decrease may be related to the decrease in the particle size (Figure 5a), which can be due
11 to the decrease of the oligomer size, by fragmentation of the oligomers. It is thus likely that
12 the oligomer aging forms more volatile compounds that the SMPS does not measure. The
13 high correlation between the total aerosol mass concentration and the consumed MVK
14 observed in Figure 6 from 0 to 50 min, allows for the determination of the SOA mass yield, as
15 discussed in section 3.2.3.

16 3.2.2 Influence of initial MVK concentrations

17 The influence of the initial aqueous phase concentration of MVK on the SOA formation was
18 investigated over a wide range, *i.e.* from 0.2 to 20 mM (Table 1). Not surprisingly, Figure 7
19 shows that the total aerosol mass concentration increases with increasing initial MVK
20 concentration. This observation is in very good agreement with the influence of MVK initial
21 concentration on the oligomerization process observed in the aqueous phase by Renard et al.
22 (2013). For experiments D and E, corresponding to the lowest initial MVK concentrations, the
23 SMPS and AMS signals were low, and they could be influenced by water impurities, whereas
24 no such influence was observed for experiments A, B and C. This is why the signal obtained
25 from the blank experiments was subtracted only for experiments D and E in Figure 7.
26 Moreover, Figure 7 clearly shows a different kinetic behavior of the SOA mass concentration
27 from the lowest initial concentration experiments (D and E), compared to the three highest
28 ones (experiments A, B and C). For experiments A, B and C, the SOA mass concentration
29 increases rapidly, reaches a maximum, and then decreases, while for experiments D and E, the
30 signal slowly increases and does not reach a maximum. This particular evolution may be due
31 to different chemical mechanisms occurring at different initial concentrations. We
32 hypothesized the predominance of oligomerization at 2 mM initial concentration and above,
33 this is further discussed in section 4.

1 The continuous increase of the particle number (shown in Figure 5a for experiment B) with
 2 reaction time was observed for all initial concentrations (experiments A to E), whereas the
 3 decrease of the size mode (in the number size distributions, after t_{max}) was observed for the
 4 three highest initial concentrations only (experiments A, B and C) and not for experiments D
 5 and E, *i.e.* only during oligomer aging.
 6 Furthermore, studies on relevant mixtures of UWSOC are in progress and could contribute to
 7 this chemistry.

8 3.2.3 SOA mass yields

9 The SOA mass yields, Y_t , were calculated at each reaction time step t from eq. 2. $Y_t = \frac{[SOA]_t}{\Delta[MVK]_t}$
 10 (eq. 2)

11 Where $\Delta[MVK]_t$ is the consumed [MVK] in mg L^{-1} at reaction time t ; and $[SOA]_t$ is the
 12 formed SOA mass at reaction time t , in mg per L of evaporated water. This term takes into
 13 account the SOA mass (M_{SMPS}) measured by the SMPS at time t (in $\mu\text{g m}^{-3}$), the atomizer flow
 14 ($F_{atomizer}$ in L m^{-3}), the dilution (f_{dil}), and the transmission efficiency in our nebulizing system
 15 (T_{eff} in %) (see Table S1).

$$16 \quad [SOA]_t = \frac{M_{SMPS} \times T_{eff}}{F_{atomizer} \times f_{dil} \times 1000} \quad \text{(eq. 3)}$$

17 ~~measured by SMPS (in mg L^{-1} of evaporated water, considering the dilution flow and the~~
 18 ~~transmission efficiency in our nebulizing system, see Table S1); and $\Delta[MVK]_t$ is the~~
 19 ~~consumed [MVK] in mg L^{-1} at reaction time t .~~

20 The yields obtained at t_{max} for experiments A, B and C are shown in Table 3. Although the
 21 total SOA mass (at t_{max}) increases linearly with the initial concentration for these three
 22 experiments, the yields are statistically identical as well as their H/C and O/C ratios. Due to
 23 the very large uncertainties affected to our yield determinations (see below), it is not possible
 24 to use these data (Table 2 and 3) to provide any interpretation on the possible effect of initial
 25 concentrations on the yields. In contrast, the O/C and H/C ratios clearly show statistically
 26 stable values when the total particle mass increases from 100 to 900 $\mu\text{g/m}^3$ (Table 3). It is thus
 27 likely that the total mass loading does not influence the relative oxygenation of the SOA
 28 produced (at t_{max}) under our experimental conditions.

29 Although the particle mass loadings (M_{SMPS}) were accurately measured, our yield
 30 determinations were affected by large uncertainties due to the estimation of the transmission
 31 efficiency in our nebulizing system (see supplementary information 1).

1 In order to confirm these yields' values, another method was tested for experiment A at 90
2 min of reaction (*i.e.* close to t_{max}). Preparative chromatography was performed using UPLC,
3 where small molecules were separated from the oligomers using a divert valve (at retention
4 times lower than 2 min.). The solution containing oligomers was accumulated, concentrated
5 and analyzed using a TOC analyzer. From the carbon mass, we deduced the total mass using
6 the H/C and O/C ratios given by the AMS. The yield was then directly calculated from the
7 total mass of sample (in mg L⁻¹) divided by the mass of consumed MVK at the same reaction
8 time. A yield of 59 ± 5 % (in mass) was obtained with this method at 90 min of reaction, thus
9 statistically similar from the one obtained by the nebulizing method (70 ± 50 %) at t_{max} .
10 These yields are significantly higher than those obtained by Liu et al. (2012) who obtained
11 yields up to 9.9 % under similar experimental conditions as ours. It is important to note that
12 these values were obtained assuming all the particle densities were 1 g cm⁻³ in Liu et al.
13 (2012), and also the transmission efficiency of the nebulizing system was calibrated with
14 NaCl solutions. However, it is likely that succinic acid or ammonium nitrate are more
15 adequate for the calibration, and we show (in the supplementary information 1) that the
16 transmission efficiency of NaCl solutions are significantly different from the two other
17 solutions. The nebulizing system was slightly different, with a teflon bag in Liu et al. (2012)
18 that could enable i) larger amounts of wall losses for organic particles as compared to the
19 system presented here; but ii) longer particle residence times, leaving more time for gas-
20 particle equilibrium than in our system. However, the control experiment using preparative
21 chromatography confirms the high yield value obtained here, independent on the nebulizing
22 system and its calibration. The different yields obtained here as compared to the study by Liu
23 et al. (2012) may be due to the different irradiation Xe lamp used: 300 W (with a pyrex filter)
24 in Liu et al., 2012, and 1000 W (with a ASTM 490 AM 0 filter) in the present study. The
25 influence of the lamp spectra on SOA mass yields of other systems (gas phase photooxidation
26 of biogenic and anthropogenic precursors) have been previously observed in atmospheric
27 simulation chambers (Bregonzio-Rozier et al., 2014). We verified, using a spectroradiometer
28 (SR-501, LOT-Oriel), that the spectral irradiance of the 300W and the 1000W Xe lamps at λ
29 ≥ 400 nm represent respectively half and twice the solar irradiance intensity at sea level, for a
30 48.3° zenith angle (Figure S1). Due to the high variability of the irradiance in the atmosphere
31 at $\lambda \geq 400$ nm (as shown by the Tropospheric Ultraviolet and Visible Radiation Model
32 http://cprm.acd.ucar.edu/Models/TUV/Interactive_TUV/), both lamps can be seen as
33 representative of the natural irradiance in this wavelength range. However at 300 nm, the

1 [spectral irradiance of the 1000W Xe lamp is 7 and 9 times higher than that of the direct solar](#)
2 [irradiance \(for a 48.3° zenith angle\) and the 300W Xe lamp respectively \(Figure S1\). This](#)
3 [part of the spectrum is essential for photochemistry, and may induce different photochemical](#)
4 [processes: we verified that](#) we observed the same series of oligomers as in Liu et al. (2012),
5 but with different relative intensities (Figure S2). [The different spectral irradiance of the lights](#)
6 [used at 300 nm may be the reason for the different yields obtained, but it needs to be](#)
7 [confirmed by a thorough study of the influence of the spectral irradiance \(in the UV\) on the](#)
8 [oligomer mass yields.](#)

9 It is interesting to note that the yields and densities obtained in the present study are in the
10 same range as those of a similar study with a different precursor, *i.e.* glycolaldehyde [and a](#)
11 [different irradiation system even more intense in the UV \(*i.e.* a 254-nm mercury lamp\)](#) (Ortiz-
12 Montalvo et al., 2012). They reported aqSOA yields for oxidation products of glycolaldehyde
13 (1 mM) which decrease gradually with reaction time from about 120% to 50%; while the
14 calculated densities increase from 1.3 to 1.6 g cm⁻³.

15 4. Discussion

16 This section discusses the results obtained on [the aging of the reaction products of MVK·OH](#)
17 [experiments and the related oxidation processes](#) in two ways. First, [the competition](#) between
18 functionalization and [oligomerization and the subsequent aging according to the initial](#)
19 [concentration of MVK is discussed; and second, a Van Krevelen diagram, \(*i.e.* H/C vs O/C](#)
20 [ratios\) of the obtained SOA is presented to study the oligomer aging process and compared](#)
21 [with oxidation processes observed by Ng et al. \(2011\) to previous studies.](#)

22 4.1 MVK functionalization versus oligomerization: influence of initial concentration

23 [In order to compare our work with the aging of organic aerosol in the atmosphere compiled](#)
24 [by Ng et al. \(2010\), we used the AMS data, and in particular, the development of the two](#)
25 [dominant fragments, \$m/z\$ 44 \(\$\text{CO}_2^+\$ \) and \$m/z\$ 43 \(mostly \$\text{C}_2\text{H}_3\text{O}^+\$ \), observed in our study. More](#)
26 [precisely, we focused on the ratio of \$m/z\$ 44 and \$m/z\$ 43 to total organic aerosol, \$f_{44}\$ and \$f_{43}\$,](#)
27 [respectively.](#)

28 In Ng et al. (2010), low volatility oxygenated organic aerosol (LV-OOA) has higher f_{44} than
29 semi-volatile oxygenated organic aerosol (SV-OOA) which in turn has higher f_{43} values.
30 [Despite the very different conditions, it is interesting to compare our aging data with those](#)
31 [compiled from field studies and other aqueous phase experiments.](#) Figure 8 compares our f_{44}
32 versus f_{43} values to those provided in the compilation by Ng et al. (2010) [as well as the](#)

1 | [nebulization data by Lee et al., \(2011a\)](#). It is clear from this figure that the SOA composition
2 and its evolution highly depend on the initial MVK concentration. For the three highest initial
3 concentrations (experiments A, B and C), oligomerization takes place with the formation of
4 oligomers containing repetitive carbonyl functions such as those identified in the aqueous
5 phase (Figure 2c), inducing an important increase of f_{43} and a simultaneous decrease of f_{44} ,
6 roughly up to t_{max} . After t_{max} , most of the initial MVK is consumed, slowing down the
7 oligomerization process, and an important decrease of f_{43} and a simultaneous increase of f_{44} is
8 observed, likely due to oligomer aging, as detailed (for experiment B) in section 3.1. At lower
9 initial MVK concentrations (experiments D and E), oligomerization seems much less
10 important and oxidation is the dominant process, as evidenced by the continuous increase of
11 f_{44} . It can thus be suggested that, at these lower initial concentrations, functionalization
12 dominates over oligomerization, and the aerosol is mainly composed of low-volatility organic
13 acid and not of MVK-oligomers.

14 This observation is strengthened by the comparison of our results with those of previous
15 studies. Zhang et al., (2010) performed aqueous phase $\cdot\text{OH}$ oxidation of MVK (0.2 mM initial
16 concentration), and observed the formation of functionalization products, *i.e.* formaldehyde,
17 glyoxal, methylglyoxal, pyruvic, oxalic, formic, acetic, and malonic acids. Furthermore, for
18 experiments D and E ($[\text{MVK}]_0 \leq 0.5$ mM), our f_{44} - f_{43} plots are similar to those obtained using
19 a similar set-up, starting from pinonic acid, glyoxal and glyoxylic acid at similar and higher
20 initial concentrations (Lee et al., 2011a; Lee et al., 2011b). In particular, starting at 3 mM of
21 glyoxal, Lee et al., 2011b obtained similar f_{44} - f_{43} plots as our experiments performed at much
22 lower initial concentrations ($[\text{MVK}]_0 \leq 0.5$ mM), thus showing that the concentration is not
23 the only important parameter in oligomerization processes, but the chemical nature of the
24 precursor is also fundamental.

25 | MVK oligomerization occurs *via* saturation of the vinyl group (Renard et al., 2013). [The](#)
26 [resulting radical monomer is stabilized by the resonance effect with the adjacent carbonyl](#)
27 [group](#) ~~The carbonyl linkage leads to stabilization of the monomer and~~ this stabilization
28 decreases the enthalpy of polymerization (Odian 2004) and hence facilitates the
29 oligomerization in the aqueous phase compared to other molecules.

31 4.2 Oligomer aging processes

32 The Van Krevelen diagram (Figure 9) shows a significant increase of O/C and a significant
33 decrease of H/C with reaction time after t_{max} . When oligomerization is the dominating

1 process, almost no changes are observed in the van Krevelen diagram: the H/C and O/C
2 values are confined in a restricted circle until t_{max} . The atomic ratios for H/C and O/C of MVK
3 and the oligomers (with a degree of polymerization (DP) of 5) identified by Renard et al.
4 (2013) are also reported in this diagram. MVK, oligomers and the nebulized solutions until
5 t_{max} are confined in a circle that highlights the similarity of their structures.
6 After that time, the values of O/C (H/C respectively) increase (decrease respectively) out of
7 the circle, thus denoting an oligomer aging process. Changes in functionality of organic
8 aerosol are traced in this diagram along a line, which slope is -0.6. A very similar slope value
9 (-0.5) was interpreted by Ng et al. (2011) as a COOH group addition to the site of a C-C bond
10 cleavage, thus suggesting that the oligomer aging process proceeds *via* fragmentation. This is
11 also suggested by the time evolution of the particle number size distributions (Figure 5a: see
12 section 3.2.1). While a continuous increase of the particle number with reaction time was
13 observed for all initial concentrations (experiments A to E), a significant decrease of the size
14 mode was observed after t_{max} for the highest concentrations only (experiments A, B and C),
15 *i.e.* during oligomer aging. This size mode decrease was also correlated with a decreasing
16 total mass (Figure 5b). These observations, added to the fact that f_{44} increases during oligomer
17 aging, indicate that the oligomer aging proceeds *via* fragmentation processes that generate
18 smaller (or more volatile) and more acidic compounds.
19 The formation of carboxylic acids in the aqueous phase was monitored during the course of
20 the reaction. In good agreement with Zhang et al. (2010), small volatile monocarboxylic acids
21 such as acetic, formic and pyruvic acids were formed as primary reaction products from MVK
22 reactivity. We further observed the formation of diacids as secondary or tertiary reaction
23 products, such as oxalic, malonic, succinic (Figure 10) malic and tartaric acids (not
24 quantified). Finally, the formation of these diacids started at t_{max} , and was correlated to the
25 increase of the AMS m/z 44 (CO_2^+) signal observed from the nebulized solutions. It is thus
26 likely that the oligomer aging proceed *via* fragmentation (by $\cdot\text{OH}$ oxidation and/or
27 photolysis), leading to the formation of smaller partially oxidized products (*i.e.* hydroxyacids
28 or ketoacids such as those identified by Jaoui et al., 2006), which, in turn are oxidized into
29 stable diacids.

30 **5. Atmospheric implications**

31 Considering the results obtained here on oligomer formation and aging from MVK at varying
32 initial concentrations together with those obtained by previous studies on the identification of

1 the low-molecular-weight compounds products of the reaction (Zhang et al., 2010), a general
2 scheme of the potential atmospheric fate of MVK in the aqueous phase is shown on Figure 11.
3 MVK \cdot OH-oxidation undergoes kinetic competition between functionalization and
4 oligomerization, depending on the precursor initial concentration. At 2 mM of MVK and
5 above this concentration, oligomerization dominates over functionalization. At these
6 concentrations, \cdot OH-oxidation of MVK forms oligomers that are SV-OOA, with low O/C
7 (lower than 0.50) and high f_{43} . Oligomers are then fragmented, *via* unidentified intermediates
8 that have the properties of LV-OOA (with increasing O/C and decreasing H/C, Figure 9)
9 which then form organic diacids. For lower initial MVK concentrations (< 2 mM),
10 oligomerization is not the major process, and functionalization dominates, ending into small
11 carbonyls, dicarbonyls and acids that were identified by Zhang et al., (2010) (Figure 11).
12 Among the atmospherically relevant alkenoic alcohols, acids, ketones and aldehydes (i.e.
13 UWSOC), although MVK is one of the most abundant species, it is one of the most volatile
14 ($P_{\text{sat}} = 10^{-5} - 0.1$ atm, with $P_{\text{sat(MVK)}} = 0.1$ atm at 25°C; Asher and Pankow 2006), and one of
15 the least soluble compounds ($K_{\text{H}} = 1 - 10^3$ M atm⁻¹, with $K_{\text{H(MVK)}} = 41$ M atm⁻¹ at 25°C; Iraci
16 et al., 1999). The atmospheric impacts of the processes shown here should thus be very
17 limited for MVK alone. However, the oligomerization mechanism undergone by MVK occurs
18 *via* saturation of the vinyl group (Renard et al., 2013), and the resulting radical monomer is
19 stabilized by the resonance effect with the adjacent carbonyl group thus decreasing the
20 enthalpy of polymerization facilitating the oligomerization in the aqueous phase compared to
21 other molecules. More generally, conjugation of the C=C with substituents such as the
22 benzene ring (styrene and *a*-methylstyrene), and alkene double bond (butadiene and isoprene),
23 the carbonyl linkage (acrylic acid, methyl acrylate, methyl methacrylate), and the nitrile group
24 (acrylonitrile) similarly leads to stabilization of the monomer and decreases enthalpies of
25 polymerization (Odian 2004). It is thus likely that a large number of atmospherically relevant
26 molecules can follow the same process either in the bulk or at the wet aerosol interface
27 (Kameel et al., 2013; Kameel et al., 2014). In this context, our results suggest that this class of
28 compounds can impact the aerosol composition, and contribute to aqSOA formation upon
29 water evaporation. The corresponding aqSOA mass yields seem to depend on the spectral
30 irradiance of the light used to initiate the photochemistry, but further studies are needed to
31 confirm this point. Finally, the aging of the oligomers formed could be an explanation (at least
32 in part) for the presence the diacids (such as oxalic, malonic and succinic acids) observed in
33 the ambient aerosol (Legrand et al., 2007; Kawamura et al., 2010). In Part 2 of this study, the

1 atmospheric relevance of these processes is explored by means of multiphase box model
2 studies.

3 ~~Figure 11 shows potential atmospheric fate of MVK in the aqueous phase. MVK \cdot OH-~~
4 ~~oxidation undergoes kinetic competition between functionalization and oligomerization,~~
5 ~~depending on the precursor initial concentration. At 2mM of MVK and above this~~
6 ~~concentration, oligomerization dominates over functionalization. Hence, at these~~
7 ~~concentrations, \cdot OH oxidation of MVK forms oligomers that are SV-OOA, with low O/C~~
8 ~~(lower than 0.50) and high f_{43} . Oligomers are then fragmented, via unidentified intermediates~~
9 ~~that have the properties of LV-OOA (with increasing O/C and decreasing H/C, Fig. 9) which~~
10 ~~then result in diacids. For lower initial MVK concentrations, the oligomerization is not the~~
11 ~~major process, and functionalization dominates, ending into small carbonyls, dicarbonyls and~~
12 ~~acids (Fig. 11).~~

13 ~~Recently, we have shown in a previous study (Renard et al., 2013) the mechanism of~~
14 ~~oligomerization of MVK (methyl vinyl ketone), and suggested that UWSOC might efficiently~~
15 ~~form SOA in wet aerosol particles, even for weakly soluble ones like MVK. This latter~~
16 ~~undergoes radical oligomerization, which is extremely fast and is able to form~~
17 ~~macromolecules as high as 1800amu in polluted fogs and wet aerosols. Radical~~
18 ~~oligomerization occurs in wet aerosols and in most polluted fogs (Lim et al., 2013; Renard et~~
19 ~~al., 2013). This result, added to the fact that the lifetime of wet aerosols in the atmosphere are~~
20 ~~several days, suggests the relevance of radical oligomerization of UWSOC in the atmosphere.~~
21 ~~Besides, the aging of these oligomers could be an explanation for the presence of a part of the~~
22 ~~diacids observed in aerosol.~~

23 ~~In Part 2 of this study, the atmospheric relevance of oligomerization will be explored by~~
24 ~~means of box model studies and comparison to other SOA formation pathways from MVK~~
25 ~~(and related compounds).~~

26
27 *Acknowledgements.* We thank the National Research Agency ANR (project CUMULUS
28 ANR-2010-BLAN-617-01), AXA insurances, Région Rhone-Alpes (CIBLE program) and
29 CNRS-INSU (LEFE-CHAT AtmOrbitrap project) for funding this research. We also thank
30 Barbara Ervens (CIRES, University of Colorado, Boulder and Chemical Sciences Division,
31 National Oceanic and Atmospheric Administration (NOAA), Boulder, CO, USA) for valuable
32 scientific discussions on this topic; Etienne Quivet (Aix-Marseille university, Laboratory of
33 Chemistry of Environment) for proofreading and Assia Smaani (Aix-Marseille university,

- 1 Laboratory of Chemistry of Environment) for contributing to the experimental work on MVK
- 2 $\cdot\text{OH}$ -oxidation experiments.
- 3

References

- 1
- 2 Aiken, A. C., DeCarlo, P. F., Kroll, J. H., Worsnop, D. R., Huffman, J. A., Docherty, K. S.,
3 Ulbrich, I. M., Mohr, C., Kimmel, J. R., Sueper, D., Sun, Y., Zhang, Q., Trimborn, A.,
4 Northway, M., Ziemann, P. J., Canagaratna, M. R., Onasch, T. B., Alfarra, M. R., Prevot,
5 A. S. H., Dommen, J., Duplissy, J., Metzger, A., Baltensperger, U. and Jimenez, J. L.: O/C
6 and OM/OC Ratios of Primary, Secondary, and Ambient Organic Aerosols with High-
7 Resolution Time-of-Flight Aerosol Mass Spectrometry, *Environmental Science &*
8 *Technology*, 42(12), 4478–4485, doi:10.1021/es703009q, 2008.
- 9 Aljawhary, D., Lee, A. K. Y. and Abbatt, J. P. D.: High-resolution chemical ionization mass
10 spectrometry (ToF-CIMS): application to study SOA composition and processing,
11 *Atmospheric Measurement Techniques*, 6(11), 3211–3224, doi:10.5194/amt-6-3211-2013,
12 2013.
- 13 Altieri, K. E., Carlton, A. G., Lim, H.-J., Turpin, B. J. and Seitzinger, S. P.: Evidence for
14 Oligomer Formation in Clouds: Reactions of Isoprene Oxidation Products, *Environmental*
15 *Science & Technology*, 40(16), 4956–4960, doi:10.1021/es052170n, 2006.
- 16 Altieri, K. E., Seitzinger, S. P., Carlton, A. G., Turpin, B. J., Klein, G. C. and Marshall, A. G.:
17 Oligomers formed through in-cloud methylglyoxal reactions: Chemical composition,
18 properties, and mechanisms investigated by ultra-high resolution FT-ICR mass
19 spectrometry, *Atmospheric Environment*, 42(7), 1476–1490,
20 doi:10.1016/j.atmosenv.2007.11.015, 2008.
- 21 Arakaki, T., Anastasio, C., Kuroki, Y., Nakajima, H., Okada, K., Kotani, Y., Handa, D.,
22 Azechi, S., Kimura, T., Tsuchi, A. and Miyagi, Y.: A General Scavenging Rate Constant
23 for Reaction of Hydroxyl Radical with Organic Carbon in Atmospheric Waters,
24 *Environmental Science & Technology*, 130718140737000, doi:10.1021/es401927b, 2013.
- 25 Asher, W. E. and Pankow, J. F.: Vapor pressure prediction for alkenoic and aromatic organic
26 compounds by a UNIFAC-based group contribution method, *Atmospheric Environment*,
27 40(19), 3588–3600, doi:10.1016/j.atmosenv.2005.12.004, 2006.
- 28 Blando, J. D. and Turpin, B. J.: Secondary organic aerosol formation in cloud and fog
29 droplets: a literature evaluation of plausibility, 2000, 34(10), 1623–1632,
30 doi:10.1016/S1352-2310(99)00392-1, 2000.
- 31 Brégonzio-Rozier, L., Siekmann, F., Giorio, C., Pangui, E., Morales, S. B., Temime-Roussel,
32 B., Gratién, A., Michoud, V., Ravier, S., Tapparo, A., Monod, A. and Doussin, J.-F.:
33 Gaseous products and Secondary Organic Aerosol formation during long term oxidation of
34 isoprene and methacrolein, *Atmospheric Chemistry and Physics Discussions*, 14(16),
35 22507–22545, doi:10.5194/acpd-14-22507-2014, 2014.
- 36 Canagaratna, M. R., Jayne, J. T., Jimenez, J. L., Allan, J. D., Alfarra, M. R., Zhang, Q.,
37 Onasch, T. B., Drewnick, F., Coe, H., Middlebrook, A., Delia, A., Williams, L. R.,
38 Trimborn, A. M., Northway, M. J., DeCarlo, P. F., Kolb, C. E., Davidovits, P. and
39 Worsnop, D. R.: Chemical and microphysical characterization of ambient aerosols with the
40 aerodyne aerosol mass spectrometer, *Mass Spectrometry Reviews*, 26(2), 185–222,
41 doi:10.1002/mas.20115, 2007.
- 42 Carlton, A. G. and Turpin, B. J.: Particle partitioning potential of organic compounds is
43 highest in the Eastern US and driven by anthropogenic water, *Atmospheric Chemistry and*
44 *Physics*, 13(20), 10203–10214, doi:10.5194/acp-13-10203-2013, 2013.

- 1 Carlton, A. G., Turpin, B. J., Altieri, K. E., Seitzinger, S., Reff, A., Lim, H.-J. and Ervens, B.:
2 Atmospheric oxalic acid and SOA production from glyoxal: Results of aqueous
3 photooxidation experiments, *Atmospheric Environment*, 41(35), 7588–7602,
4 doi:10.1016/j.atmosenv.2007.05.035, 2007.
- 5 Carlton, A. G., Turpin, B. J., Lim, H.-J., Altieri, K. E. and Seitzinger, S.: Link between
6 isoprene and secondary organic aerosol (SOA): Pyruvic acid oxidation yields low volatility
7 organic acids in clouds, *Geophysical Research Letters*, 33(6), doi:10.1029/2005GL025374,
8 2006.
- 9 Carlton, A. G., Wiedinmyer, C. and Kroll, J. H.: A review of Secondary Organic Aerosol
10 (SOA) formation from isoprene, *Atmospheric Chemistry and Physics*, 9(14), 4987–5005,
11 2009.
- 12 Daumit, K. E., Carrasquillo, A. J., Hunter, J. F. and Kroll, J. H.: Laboratory studies of the
13 aqueous-phase oxidation of polyols: submicron particles vs. bulk aqueous solution,
14 *Atmospheric Chemistry and Physics*, 14(19), 10773–10784, doi:10.5194/acp-14-10773-
15 2014, 2014.
- 16 DeCarlo, P. F., Dunlea, E. J., Kimmel, J. R., Aiken, A. C., Sueper, D., Crouse, J., Wennberg,
17 P. O., Emmons, L., Shinzuka, Y., Clarke, A. and others: Fast airborne aerosol size and
18 chemistry measurements with the high resolution aerosol mass spectrometer during the
19 MILAGRO Campaign, *Atmos. Chem. Phys. Discuss*, 7(18), 269–18, 2007.
- 20 DeCarlo, P. F., Kimmel, J. R., Trimborn, A., Northway, M. J., Jayne, J. T., Aiken, A. C.,
21 Gonin, M., Fuhrer, K., Horvath, T., Docherty, K. S., Worsnop, D. R. and Jimenez, J. L.:
22 Field-Deployable, High-Resolution, Time-of-Flight Aerosol Mass Spectrometer,
23 *Analytical Chemistry*, 78(24), 8281–8289, doi:10.1021/ac061249n, 2006.
- 24 Docherty, K. S., Jaoui, M., Corse, E., Jimenez, J. L., Offenberg, J. H., Lewandowski, M. and
25 Kleindienst, T. E.: Collection Efficiency of the Aerosol Mass Spectrometer for Chamber-
26 Generated Secondary Organic Aerosols, *Aerosol Science and Technology*, 47(3), 294–309,
27 doi:10.1080/02786826.2012.752572, 2013.
- 28 Donahue, N. M., Epstein, S. A., Pandis, S. N. and Robinson, A. L.: A two-dimensional
29 volatility basis set: 1. organic-aerosol mixing thermodynamics, *Atmospheric Chemistry
30 and Physics*, 11(7), 3303–3318, doi:10.5194/acp-11-3303-2011, 2011.
- 31 Epstein, S. A., Tapavicza, E., Furche, F. and Nizkorodov, S. A.: Direct photolysis of carbonyl
32 compounds dissolved in cloud and fog~droplets, *Atmospheric Chemistry and Physics*,
33 13(18), 9461–9477, doi:10.5194/acp-13-9461-2013, 2013.
- 34 Ervens, B., Turpin, B. J. and Weber, R. J.: Secondary organic aerosol formation in cloud
35 droplets and aqueous particles (aqSOA): a review of laboratory, field and model studies,
36 *Atmospheric Chemistry and Physics*, 11(21), 11069–11102, doi:10.5194/acp-11-11069-
37 2011, 2011.
- 38 Ervens, B. and Volkamer, R.: Glyoxal processing by aerosol multiphase chemistry: towards a
39 kinetic modeling framework of secondary organic aerosol formation in aqueous particles,
40 *Atmospheric Chemistry and Physics*, 10(17), 8219–8244, doi:10.5194/acp-10-8219-2010,
41 2010.
- 42 Guenther, A., Karl, T., Harley, P., Wiedinmyer, C., Palmer, P. I., Geron, C. and others:
43 Estimates of global terrestrial isoprene emissions using MEGAN (Model of Emissions of
44 Gases and Aerosols from Nature), *Atmospheric Chemistry and Physics*, 6(11), 3181–3210,
45 2006.

- 1 Haddad, I. E., Liu, Y., Nieto-Gligorovski, L., Michaud, V., Temime-Roussel, B., Quivet, E.,
2 Marchand, N., Sellegri, K. and Monod, A.: In-cloud processes of methacrolein under
3 simulated conditions—Part 2: Formation of secondary organic aerosol, *Atmospheric*
4 *Chemistry and Physics*, 9(14), 5107–5117, 2009.
- 5 Hallquist, M., Wenger, J., Baltensperger, U., Rudich, Y., Simpson, D., Claeys, M., Dommen,
6 J., Donahue, N. M., George, C., Goldstein, A. H., Hamilton, J. V., Herrmann, H.,
7 Hoffmann, T., Iinuma, Y., Jang, M., Jenkin, M. E., Jimenez, J. L., Kiendler-Scharr, A.,
8 Maenhaut, W., McFiggans, G. B., Mentel, T. F., Monod, A., Prevot, A. S. H., Seinfeld, J.
9 H., Surratt, J. D., Szmigielski, R. and wild: The formation, properties and impact of
10 secondary organic aerosol: current and emerging issues, *Atmospheric Chemistry and*
11 *Physics*, 9(14), 5155–5236, doi:10.5194/acp-9-5155-2009, 2009.
- 12 Herrmann, H., Hoffmann, D., Schaefer, T., Brüner, P. and Tilgner, A.: Tropospheric
13 Aqueous-Phase Free-Radical Chemistry: Radical Sources, Spectra, Reaction Kinetics and
14 Prediction Tools, *ChemPhysChem*, 11(18), 3796–3822, doi:10.1002/cphc.201000533,
15 2010.
- 16 Hobby, K.: A novel method of isotope prediction applied to elemental composition analysis,
17 2005.
- 18 Iraci, L. T., Baker, B. M., Tyndall, G. S. and Orlando, J. J.: Measurements of the Henry's law
19 coefficients of 2-methyl-3-buten-2-ol, methacrolein, and methylvinyl ketone, *Journal of*
20 *atmospheric chemistry*, 33(3), 321–330, 1999.
- 21 Jaoui, M., Corse, E., Kleindienst, T. E., Offenberg, J. H., Lewandowski, M. and Edney, E. O.:
22 Analysis of Secondary Organic Aerosol Compounds from the Photooxidation of d -
23 Limonene in the Presence of NO X and their Detection in Ambient PM 2.5, *Environmental*
24 *Science & Technology*, 40(12), 3819–3828, doi:10.1021/es052566z, 2006.
- 25 Jimenez, J. L., Canagaratna, M. R., Donahue, N. M., Prevot, A. S. H., Zhang, Q., Kroll, J. H.,
26 DeCarlo, P. F., Allan, J. D., Coe, H., Ng, N. L., Aiken, A. C., Docherty, K. S., Ulbrich, I.
27 M., Grieshop, A. P., Robinson, A. L., Duplissy, J., Smith, J. D., Wilson, K. R., Lanz, V.
28 A., Hueglin, C., Sun, Y. L., Tian, J., Laaksonen, A., Raatikainen, T., Rautiainen, J.,
29 Vaattovaara, P., Ehn, M., Kulmala, M., Tomlinson, J. M., Collins, D. R., Cubison, M. J.,
30 E., Dunlea, J., Huffman, J. A., Onasch, T. B., Alfarra, M. R., Williams, P. I., Bower, K.,
31 Kondo, Y., Schneider, J., Drewnick, F., Borrmann, S., Weimer, S., Demerjian, K., Salcedo,
32 D., Cottrell, L., Griffin, R., Takami, A., Miyoshi, T., Hatakeyama, S., Shimono, A., Sun, J.
33 Y., Zhang, Y. M., Dzepina, K., Kimmel, J. R., Sueper, D., Jayne, J. T., Herndon, S. C.,
34 Trimborn, A. M., Williams, L. R., Wood, E. C., Middlebrook, A. M., Kolb, C. E.,
35 Baltensperger, U. and Worsnop, D. R.: Evolution of Organic Aerosols in the Atmosphere,
36 *Science*, 326(5959), 1525–1529, doi:10.1126/science.1180353, 2009.
- 37 Kameel, F. R., Hoffmann, M. R. and Colussi, A. J.: OH Radical-Initiated Chemistry of
38 Isoprene in Aqueous Media. Atmospheric Implications, *The Journal of Physical Chemistry*
39 *A*, 117(24), 5117–5123, doi:10.1021/jp4026267, 2013.
- 40 Kameel, F. R., Riboni, F., Hoffmann, M. R., Enami, S. and Colussi, A. J.: Fenton Oxidation
41 of Gaseous Isoprene on Aqueous Surfaces, *The Journal of Physical Chemistry C*,
42 140725063829009, doi:10.1021/jp505010e, 2014.
- 43 Kanakidou, M., Seinfeld, J. H., Pandis, S. N., Barnes, I., Dentener, F. J., Facchini, M. C.,
44 Dingenen, R. V., Ervens, B., Nenes, A., Nielsen, C. J. and others: Organic aerosol and
45 global climate modelling: a review, *Atmospheric Chemistry and Physics*, 5(4), 1053–1123,
46 2005.

- 1 Kawamura, K., Kasukabe, H. and Barrie, L. A.: Secondary formation of water-soluble organic
2 acids and α -dicarbonyls and their contributions to total carbon and water-soluble organic
3 carbon: Photochemical aging of organic aerosols in the Arctic spring, *Journal of*
4 *Geophysical Research*, 115(D21), doi:10.1029/2010JD014299, 2010.
- 5 Kroll, J. H., Ng, N. L., Murphy, S. M., Flagan, R. C. and Seinfeld, J. H.: Secondary Organic
6 Aerosol Formation from Isoprene Photooxidation, *Environmental Science & Technology*,
7 40(6), 1869–1877, doi:10.1021/es0524301, 2006.
- 8 Kroll, J. H. and Seinfeld, J. H.: Chemistry of secondary organic aerosol: Formation and
9 evolution of low-volatility organics in the atmosphere, *Atmospheric Environment*, 42(16),
10 3593–3624, doi:10.1016/j.atmosenv.2008.01.003, 2008.
- 11 Kuwata, M., Zorn, S. R. and Martin, S. T.: Using Elemental Ratios to Predict the Density of
12 Organic Material Composed of Carbon, Hydrogen, and Oxygen, *Environmental Science &*
13 *Technology*, 46(2), 787–794, doi:10.1021/es202525q, 2012.
- 14 Lee, A. K. Y., Hayden, K. L., Herckes, P., Leaitch, W. R., Liggio, J., Macdonald, A. M. and
15 Abbatt, J. P. D.: Characterization of aerosol and cloud water at a mountain site during
16 WACS 2010: secondary organic aerosol formation through oxidative cloud processing,
17 *Atmospheric Chemistry and Physics*, 12(15), 7103–7116, doi:10.5194/acp-12-7103-2012,
18 2012.
- 19 Lee, A. K. Y., Herckes, P., Leaitch, W. R., Macdonald, A. M. and Abbatt, J. P. D.: Aqueous
20 OH oxidation of ambient organic aerosol and cloud water organics: Formation of highly
21 oxidized products: AQUEOUS OXIDATION OF AMBIENT ORGANICS, *Geophysical*
22 *Research Letters*, 38(11), n/a–n/a, doi:10.1029/2011GL047439, 2011a.
- 23 Lee, A. K. Y., Zhao, R., Gao, S. S. and Abbatt, J. P. D.: Aqueous-Phase OH Oxidation of
24 Glyoxal: Application of a Novel Analytical Approach Employing Aerosol Mass
25 Spectrometry and Complementary Off-Line Techniques, *The Journal of Physical*
26 *Chemistry A*, 115(38), 10517–10526, doi:10.1021/jp204099g, 2011b.
- 27 Lee, W., Baasandorj, M., Stevens, P. S. and Hites, R. A.: Monitoring OH-initiated oxidation
28 kinetics of isoprene and its products using online mass spectrometry, *Environmental*
29 *science & technology*, 39(4), 1030–1036, 2005.
- 30 Legrand, M., Preunkert, S., Oliveira, T., Pio, C. A., Hammer, S., Gelencsér, A., Kasper-Giebl,
31 A. and Laj, P.: Origin of C2–C5 dicarboxylic acids in the European atmosphere inferred
32 from year-round aerosol study conducted at a west-east transect, *J. Geophys. Res.*,
33 112(D23), D23S07, doi:10.1029/2006JD008019, 2007.
- 34 Lim, Y. B., Tan, Y. and Turpin, B. J.: Chemical insights, explicit chemistry, and yields of
35 secondary organic aerosol from OH radical oxidation of methylglyoxal and glyoxal in the
36 aqueous phase, *Atmospheric Chemistry and Physics*, 13(17), 8651–8667, doi:10.5194/acp-
37 13-8651-2013, 2013.
- 38 Liu, P. S. K., Deng, R., Smith, K. A., Williams, L. R., Jayne, J. T., Canagaratna, M. R.,
39 Moore, K., Onasch, T. B., Worsnop, D. R. and Deshler, T.: Transmission Efficiency of an
40 Aerodynamic Focusing Lens System: Comparison of Model Calculations and Laboratory
41 Measurements for the Aerodyne Aerosol Mass Spectrometer, *Aerosol Science and*
42 *Technology*, 41(8), 721–733, doi:10.1080/02786820701422278, 2007.
- 43 Liu, Y., Siekmann, F., Renard, P., El Zein, A., Salque, G., El Haddad, I., Temime-Roussel,
44 B., Voisin, D., Thissen, R. and Monod, A.: Oligomer and SOA formation through aqueous

- 1 phase photooxidation of methacrolein and methyl vinyl ketone, *Atmospheric Environment*,
2 49, 123–129, doi:10.1016/j.atmosenv.2011.12.012, 2012.
- 3 Miyakawa, T., Matsuzawa, R., Katayama, M. and Takegawa, N.: Reconsidering Adhesion
4 and Bounce of Submicron Particles Upon High-Velocity Impact, *Aerosol Science and*
5 *Technology*, 47(5), 472–481, doi:10.1080/02786826.2013.763895, 2013.
- 6 Ng, N. L., Canagaratna, M. R., Jimenez, J. L., Chhabra, P. S., Seinfeld, J. H. and Worsnop, D.
7 R.: Changes in organic aerosol composition with aging inferred from aerosol mass spectra,
8 *Atmospheric Chemistry and Physics*, 11(13), 6465–6474, doi:10.5194/acp-11-6465-2011,
9 2011.
- 10 Ng, N. L., Canagaratna, M. R., Zhang, Q., Jimenez, J. L., Tian, J., Ulbrich, I. M., Kroll, J. H.,
11 Docherty, K. S., Chhabra, P. S., Bahreini, R., Murphy, S. M., Seinfeld, J. H., Hildebrandt,
12 L., Donahue, N. M., DeCarlo, P. F., Lanz, V. A., Prévôt, A. S. H., Dinar, E., Rudich, Y.
13 and Worsnop, D. R.: Organic aerosol components observed in Northern Hemispheric
14 datasets from Aerosol Mass Spectrometry, *Atmospheric Chemistry and Physics*, 10(10),
15 4625–4641, doi:10.5194/acp-10-4625-2010, 2010.
- 16 Odian, G. G.: Principles of polymerization, Wiley, Hoboken, N.J. [online] Available from:
17 <http://public.eblib.com/EBLPublic/PublicView.do?ptiID=469767> (Accessed 10 October
18 2014), 2004.
- 19 Ortiz-Montalvo, D. L., Lim, Y. B., Perri, M. J., Seitzinger, S. P. and Turpin, B. J.: Volatility
20 and Yield of Glycolaldehyde SOA Formed through Aqueous Photochemistry and Droplet
21 Evaporation, *Aerosol Science and Technology*, 46(9), 1002–1014,
22 doi:10.1080/02786826.2012.686676, 2012.
- 23 Perri, M. J., Seitzinger, S. and Turpin, B. J.: Secondary organic aerosol production from
24 aqueous photooxidation of glycolaldehyde: Laboratory experiments, *Atmospheric*
25 *Environment*, 43(8), 1487–1497, doi:10.1016/j.atmosenv.2008.11.037, 2009.
- 26 Renard, P., Reed Harris, A. E., Rapf, R. J., Ravier, S., Demelas, C., Coulomb, B., Quivet, E.,
27 Vaida, V. and Monod, A.: Aqueous Phase Oligomerization of Methyl Vinyl Ketone by
28 Atmospheric Radical Reactions, *The Journal of Physical Chemistry C* [online] Available
29 from: <http://pubs.acs.org/doi/abs/10.1021/jp5065598> (Accessed 23 October 2014), 2014.
- 30 Renard, P., Siekmann, F., Gandolfo, A., Socorro, J., Salque, G., Ravier, S., Quivet, E.,
31 Clément, J.-L., Traikia, M., Delort, A.-M., Voisin, D., Vuitton, V., Thissen, R. and Monod,
32 A.: Radical mechanisms of methyl vinyl ketone oligomerization through aqueous phase
33 OH-oxidation: on the paradoxical role of dissolved molecular oxygen, *Atmospheric*
34 *Chemistry and Physics*, 13(13), 6473–6491, doi:10.5194/acp-13-6473-2013, 2013.
- 35 Spracklen, D. V., Jimenez, J. L., Carslaw, K. S., Worsnop, D. R., Evans, M. J., Mann, G. W.,
36 Zhang, Q., Canagaratna, M. R., Allan, J., Coe, H., McFiggans, G., Rap, A. and Forster, P.:
37 Aerosol mass spectrometer constraint on the global secondary organic aerosol budget,
38 *Atmospheric Chemistry and Physics*, 11(23), 12109–12136, doi:10.5194/acp-11-12109-
39 2011, 2011.
- 40 Surratt, J. D., Murphy, S. M., Kroll, J. H., Ng, N. L., Hildebrandt, L., Sorooshian, A.,
41 Szmigielski, R., Vermeylen, R., Maenhaut, W., Claeys, M., Flagan, R. C. and Seinfeld, J.
42 H.: Chemical Composition of Secondary Organic Aerosol Formed from the Photooxidation
43 of Isoprene, *The Journal of Physical Chemistry A*, 110(31), 9665–9690,
44 doi:10.1021/jp061734m, 2006.

- 1 Tan, Y., Carlton, A. G., Seitzinger, S. P. and Turpin, B. J.: SOA from methylglyoxal in clouds
2 and wet aerosols: Measurement and prediction of key products, *Atmospheric Environment*,
3 44(39), 5218–5226, doi:10.1016/j.atmosenv.2010.08.045, 2010.
- 4 Tan, Y., Lim, Y. B., Altieri, K. E., Seitzinger, S. P. and Turpin, B. J.: Mechanisms leading to
5 oligomers and SOA through aqueous photooxidation: insights from OH radical oxidation
6 of acetic acid and methylglyoxal, *Atmospheric Chemistry and Physics*, 12(2), 801–813,
7 doi:10.5194/acp-12-801-2012, 2012.
- 8 Tan, Y., Perri, M. J., Seitzinger, S. P. and Turpin, B. J.: Effects of Precursor Concentration
9 and Acidic Sulfate in Aqueous Glyoxal–OH Radical Oxidation and Implications for
10 Secondary Organic Aerosol, *Environmental Science & Technology*, 43(21), 8105–8112,
11 doi:10.1021/es901742f, 2009.
- 12 Volkamer, R., San Martini, F., Molina, L. T., Salcedo, D., Jimenez, J. L. and Molina, M. J.: A
13 missing sink for gas-phase glyoxal in Mexico City: Formation of secondary organic
14 aerosol, *Geophysical Research Letters*, 34(19), doi:10.1029/2007GL030752, 2007.
- 15 Zhang, X., Chen, Z. M. and Zhao, Y.: Laboratory simulation for the aqueous OH-oxidation of
16 methyl vinyl ketone and methacrolein: significance to the in-cloud SOA production,
17 *Atmospheric Chemistry and Physics*, 10(19), 9551–9561, doi:10.5194/acp-10-9551-2010,
18 2010.
- 19 Zhao, R., Lee, A. K. Y. and Abbatt, J. P. D.: Investigation of Aqueous-Phase Photooxidation
20 of Glyoxal and Methylglyoxal by Aerosol Chemical Ionization Mass Spectrometry:
21 Observation of Hydroxyhydroperoxide Formation, *The Journal of Physical Chemistry A*,
22 116(24), 6253–6263, doi:10.1021/jp211528d, 2012.

Exp. Name	[MVK] ₀ (mM)	[H ₂ O ₂] ₀ (mM)	MVK 90% Consumption time (min)	Aqueous phase characterization	Aerosol Characterization after nebulization
A	20	400	120		
B	5	100	50		
C	2	40	30	UPLC-ESI-MS UHPLC-UV IC-ESI-MS ^a	SMPS AMS
D	0.5	10	25		
E	0.2	4	20		

Table 1: Experimental conditions of [•]OH-oxidation of MVK in the aqueous phase. All experiments are performed at 25°C. Time 0 corresponds to MVK injection in the photoreactor (Samples taken at 0, 5, 10, 15, 30, 50, 75, 105, 150 min).

Reaction Time (min)	D_p (nm) ^a	N ($\times 10^3 \text{ cm}^{-3}$) ^a	H/C ^b	O/C ^b	ρ_{org} (g cm^{-3}) ^{b,c}	M_{SMPS} ($\mu\text{g m}^{-3}$) ^{a,d}	Yield (%) ^{a,d,e}
5	28.3 ± 0.7	90 ± 6	1.55 ± 0.02	0.28 ± 0.05	1.0 ± 0.2	10 ± 10	70 ± 80
15	38 ± 1	530 ± 30	1.55 ± 0.01	0.26 ± 0.01	1.1 ± 0.1	100 ± 20	90 ± 60
50	44 ± 1	860 ± 40	1.55 ± 0.01	0.29 ± 0.01	1.1 ± 0.1	240 ± 50	80 ± 50
105	37 ± 1	1200 ± 50	1.47 ± 0.01	0.42 ± 0.01	1.2 ± 0.2	220 ± 40	70 ± 40
150	35 ± 1	1310 ± 50	1.38 ± 0.01	0.57 ± 0.01	1.4 ± 0.2	200 ± 30	60 ± 40

Table 2: Characteristics of the aerosol formed from nebulized MVK-solutions at different reaction times for experiment B.

Values are the average of ^a three consecutive SMPS measurements, and ^b five consecutive O/C and H/C AMS measurements, and uncertainties represent the corresponding standard deviation of these averages.

^c Particle densities are calculated using the method by Kuwata et al. (2012), the associated uncertainties include the accuracy of $\pm 12\%$ stated by these authors for eq.1.

^d Mass concentration values include the corresponding aerosol densities.

^e Yield values and associated uncertainties include dilution + transmission efficiency determined for the nebulizing system (see supplementary information 1).

Exp. Name	[MVK] ₀ (mM)	t _{max} (min) ^a	ρ _{org} (g cm ⁻³) ^b	M _{SMPS} (μg m ⁻³) ^b	Yield (%) ^{b,c}	H/C ^b	O/C ^b
A	20	105	1.1 ± 0.1	900 ± 200	70 ± 50	1.54 ± 0.01	0.30 ± 0.01
B	5	50	1.1 ± 0.1	240 ± 50	80 ± 50	1.55 ± 0.01	0.29 ± 0.01
C	2	30	1.1 ± 0.1	100 ± 20	80 ± 60	1.55 ± 0.01	0.28 ± 0.01

Table 3: Overview of aerosol properties and mass yields for different initial MVK concentrations.

^a Values are given at t_{max}, corresponding to the maximum aerosol mass concentration.

^b All values and associated uncertainties are calculated as indicated in Table 2.

^c Including dilution + transmission efficiency (TE) in the nebulizing system; TE: 17.2 (±7.9) for [MVK]₀ = 2 - 20mM determined from NH₄NO₃ (see supplementary information 1).

1 **Figure 1:** Schematic overview of the aerosol generation setup
2

3 **Figure 2:** (a): Time profiles of MVK concentrations during the reaction (experiment B); and
4 the corresponding evolution of ESI-MS spectra for m/z 50 - 1200 at (b): 5 min, (c): 50 min
5 and (d): 150 min. Highlighted in red in (c) is the most intense peaks of the main series of
6 oligomers together with its related molecular structure.
7

8 **Figure 3:** Time profiles of the AMS total organic mass (red), ion fragments $C_2H_3O^+$ at m/z 43
9 (blue) and CO_2^+ m/z 44 (green) for nebulized solutions from experiment B (**a**), and the
10 corresponding evolution of AMS mass spectra (for m/z 0 - 100) for nebulized solutions
11 sampled after 5 min (**b**), 50 min (**c**) and 150 min (**d**). Values are averages of 5 consecutive
12 AMS runs, error bars represent their standard deviations.
13

14 **Figure 4:** Comparison of AMS mass spectra (in the range 100 - 200 amu) of the nebulized
15 solutions sampled from experiment B after 50 and 150 min of reaction.
16

17 **Figure 5:** Evolution of particle number (a) and mass (b) size distributions for nebulized
18 solutions sampled at different reaction times for experiment B.
19

20 **Figure 6:** Time profiles of the total aerosol mass (black diamonds) from the nebulized
21 solutions, and consumed MVK in the aqueous phase (red circles) for experiment B. ^a Values
22 represent averages of three consecutive SMPS measurements for each reaction time
23 considering the corresponding density (Table 1). Error bars represent the sum of the standard
24 deviation of these averages and the uncertainties of the density calculation. ^bMVK
25 concentrations were determined by means of UHPLC-UV, with an uncertainty of ± 2 %.
26

27 **Figure 7:** Influence of the initial MVK concentration on the evolution of the total SOA mass
28 obtained from the nebulized solutions. Values represent averages of three consecutive SMPS
29 measurements for each reaction time considering the corresponding density (Table 3). Error
30 bars represent the sum of the standard deviation of these averages and the uncertainties of the
31 density calculation. For the lowest initial concentrations (experiments D and E), blank signals
32 were subtracted, and a density of 1.1 g cm^{-3} was assumed.

1 **Figure 8:** Fractions f_{44} versus f_{43} for the nebulized solutions from experiments A, B, C, D and
2 E, as measured by the AMS are compared to ambient air LV-OOA and SV-OOA from the
3 compilation by Ng et al. (2010) (dashed black triangle), and are also compared to the
4 nebulization data by Lee et al. (2011a) (dotted grey triangle). For our experiments, the signal
5 from blank experiments was subtracted. The data are shown for experiments A, B, and C from
6 10 to 150 min of reaction, and for experiments D and E from 15 to 150 min of reaction.

7
8 **Figure 9:** Van Krevelen diagram for the nebulized solutions of experiment C, as measured by
9 the AMS. Only experiment C is shown for clarity as the data for experiments A and B are
10 stacked together with the data shown. ^a Red diamonds represent the elemental ratios of
11 oligomers with a Degree of Polymerization = 5 for the ten most abundant oligomer series
12 identified by Renard et al. (2013). The black dotted circle highlights compounds with similar
13 structures. ^b Ng et al., 2011, for details see text section 4.2.

14
15 **Figure 10 :** Time profiles of the quantified diacids in the solutions as measured by IC-ESI-
16 MS for experiment B ($[MVK]_0 = 5$ mM).

17
18 **Figure 11:** general scheme of the potential atmospheric fate of MVK in the aqueous phase. X-
19 Axis denotes volatility (\log_{10} of C^* at 298K), y-axis denotes oxidation state, approximated by
20 the O/C ratios (Jimenez et al., 2009).

21

Table 1: Experimental conditions of OH-oxidation of MVK in the aqueous phase. All experiments were performed at 25°C. Time 0 corresponds to MVK injection in the photoreactor (Samples taken at 0, 5, 10, 15, 30, 50, 75, 105, 150 min).

Exp. Name	[MVK] ₀ (mM)	[H ₂ O ₂] ₀ (mM)	MVK 90% Consumption time (min)	Aqueous phase characterization	Aerosol Characterization after nebulization
A	20	400	90	UPLC-ESI-MS UPLC-UV IC-ESI-MS	SMPS AMS
B	5	100	50		
C	2	40	30		
D	0.5	10	25	UPLC-ESI-MS UPLC-UV	SMPS AMS
E	0.2	4	20		

Table 2: Characteristics of the aerosol formed from nebulized MVK-solutions at different reaction times for experiment B.

Values are the average of ^a three consecutive SMPS measurements, and ^b five consecutive O/C and H/C AMS measurements, and uncertainties represent the corresponding standard deviation of these averages.

^c Particle densities are calculated using the method by Kuwata et al. (2012), the associated uncertainties include the accuracy of $\pm 12\%$ stated by these authors for eq.1.

^d Mass concentration values include the corresponding aerosol densities.

^e Yield values and associated uncertainties include dilution + transmission efficiency determined for the nebulizing system (see Table S1).

Reaction Time (min)	DP (nm) ^a	N ($\times 10^3 \text{ cm}^{-3}$) ^a	H/C ^b	O/C ^b	ρ^{org} (g cm^{-3}) ^{b,c}	M _{SMPS} ($\mu\text{g m}^{-3}$) ^{a,d}	Yield (%) ^{a,d,e}
5	28.3 \pm 0.7	90 \pm 6	1.55 \pm 0.02	0.28 \pm 0.05	1.0 \pm 0.2	10 \pm 10	70 \pm 80
15	38 \pm 1	530 \pm 30	1.55 \pm 0.01	0.26 \pm 0.01	1.1 \pm 0.1	100 \pm 20	90 \pm 60
50	44 \pm 1	860 \pm 40	1.55 \pm 0.01	0.29 \pm 0.01	1.1 \pm 0.1	240 \pm 50	80 \pm 50
105	37 \pm 1	1200 \pm 50	1.47 \pm 0.01	0.42 \pm 0.01	1.2 \pm 0.2	220 \pm 40	70 \pm 40
34 150	35 \pm 1	1310 \pm 50	1.38 \pm 0.01	0.57 \pm 0.01	1.4 \pm 0.2	200 \pm 30	60 \pm 40

Table 3: Overview of aerosol properties and mass yields for different initial MVK concentrations.

^a Values are given at t_{max} , corresponding to the maximum aerosol mass concentration.

^b All values and associated uncertainties are calculated as indicated in Table 2.

^c Including dilution + transmission efficiency (TE) in the nebulizing system; TE: 17.2 (± 7.9) for $[MVK]_0=2-20\text{mM}$ determined from NH_4NO_3 .

Exp. Name	$[MVK]_0$ (mM)	t_{max} (min) ^a	ρ_{org} (g cm^{-3}) ^b	M_{SMPS} ($\mu\text{g m}^{-3}$) ^b	Yield (%) ^{b,c}	H/C ^b	O/C ^b
A	20	105	1.1 ± 0.1	900 ± 200	70 ± 50	1.54 ± 0.01	0.30 ± 0.01
B	5	50	1.1 ± 0.1	240 ± 50	80 ± 50	1.55 ± 0.01	0.29 ± 0.01
C	2	30	1.1 ± 0.1	100 ± 20	80 ± 60	1.55 ± 0.01	0.28 ± 0.01

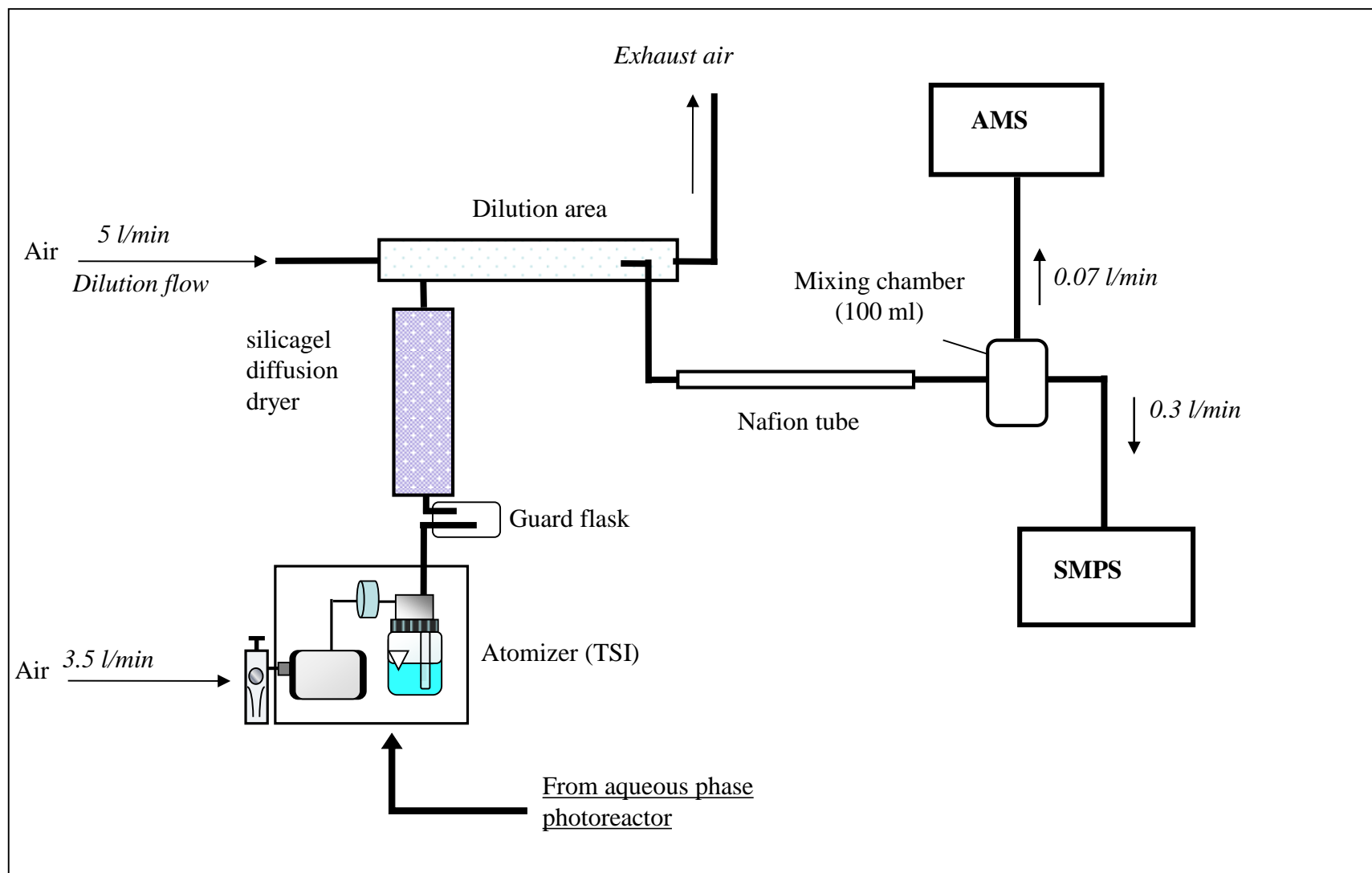


Figure 1: Schematic overview of the aerosol generation setup.

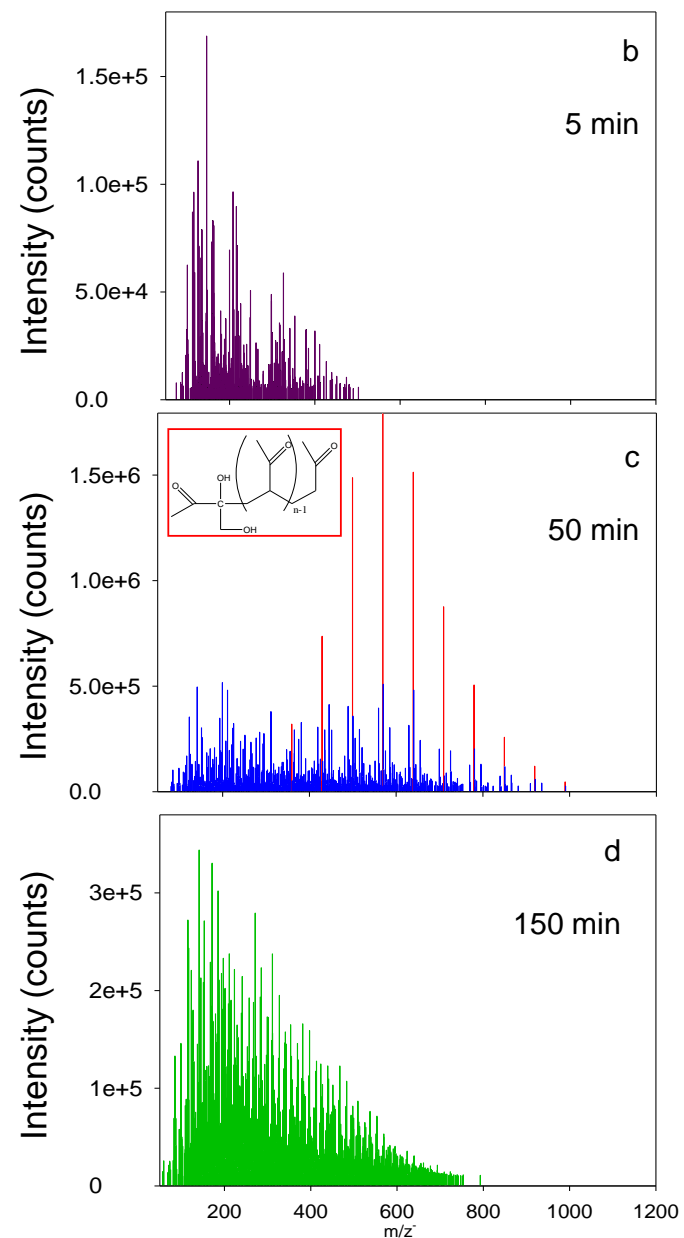
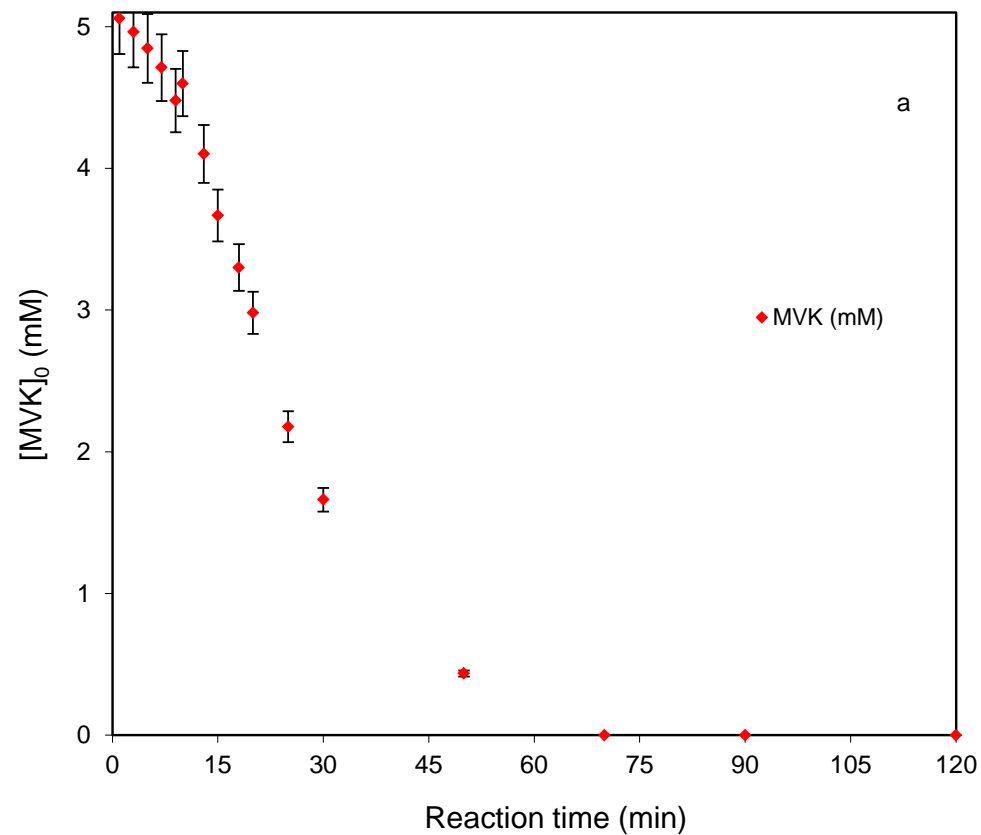


Figure 2: (a): Time profiles of MVK concentrations during the reaction (experiment B); and the corresponding evolution of ESI-MS⁻ spectra for m/z 50 - 1200 at (b): 5 min, (c): 50 min and (d): 150 min. Highlighted in red in (c), the most intense peaks of the main series of oligomers together with its related molecular structure.

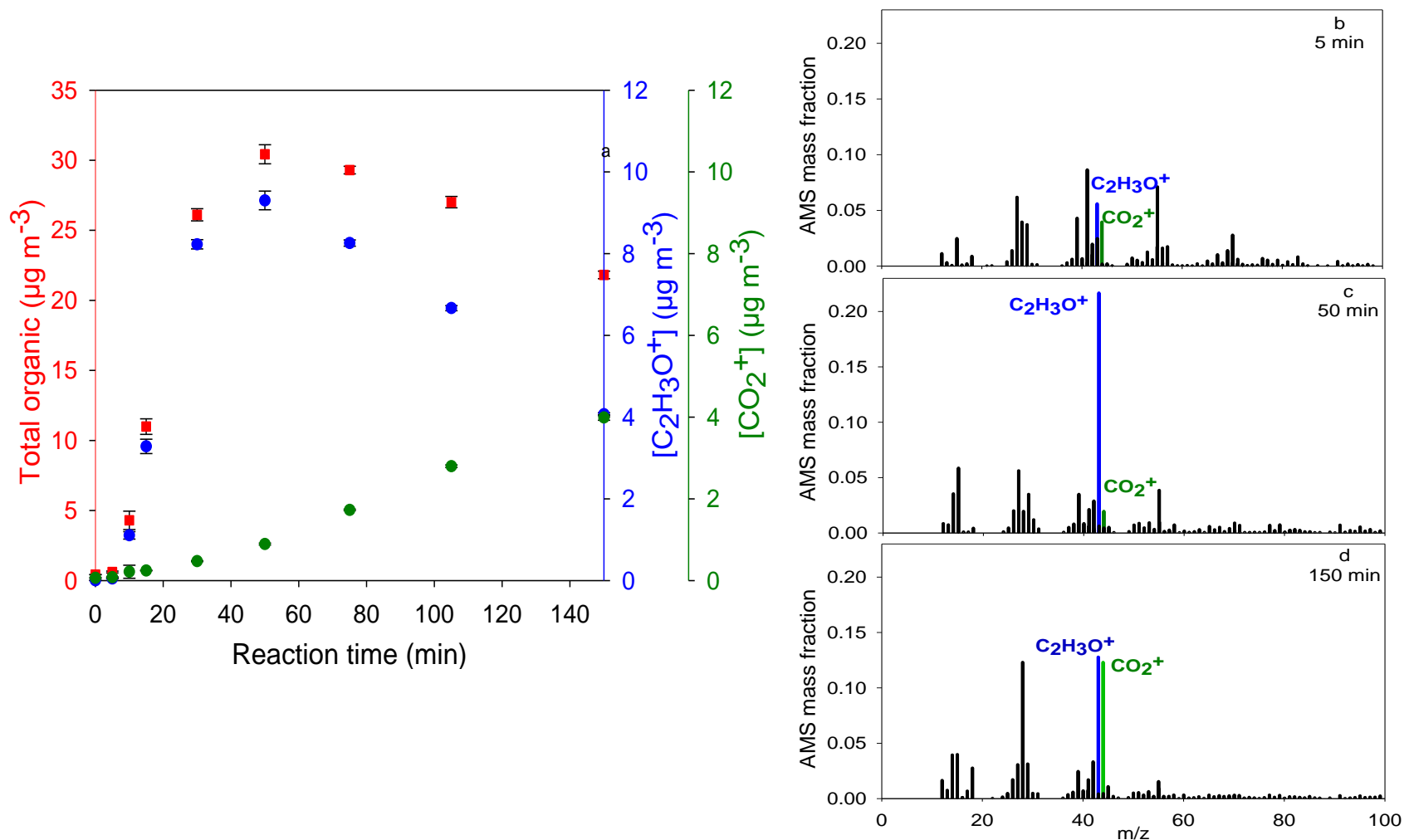


Figure 3: Time profiles of the HR-ToF-AMS total organic mass (red), ion fragments $C_2H_3O^+$ at m/z 43 (blue) and CO_2^+ m/z 44 (green) for nebulized solutions from experiment B (a), and the corresponding evolution of HR-ToF-AMS mass spectra (for m/z 0 - 100) for nebulized solutions sampled after 5 min (b), 50 min (c) and 150 min (d). Values are averages of 5 consecutive HR-ToF-AMS-runs, error bars represent their standard deviations. The AMS-mass fraction is the signal intensity contribution of each fragment to the total signal.

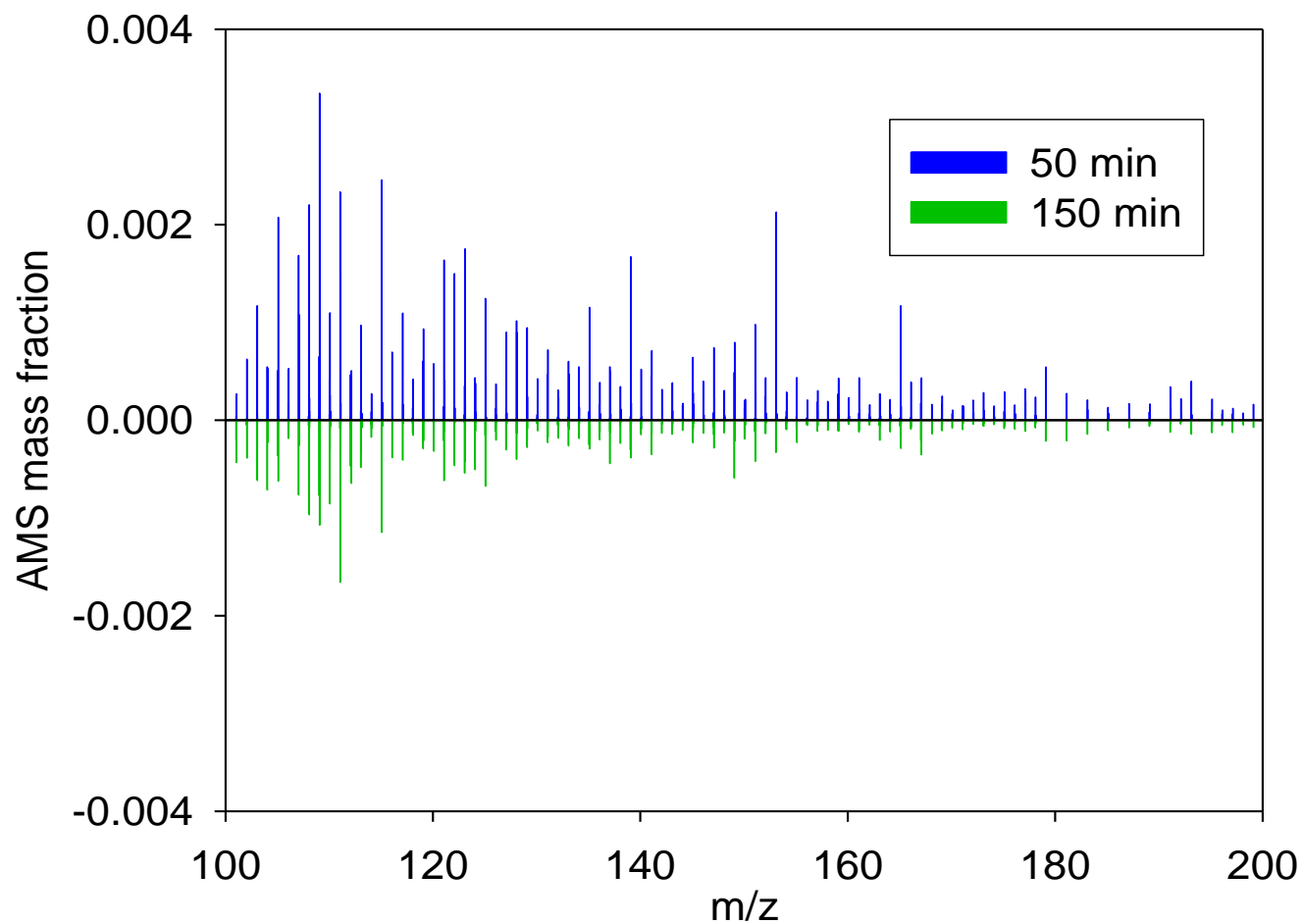


Figure 4: Comparison of HR-ToF-AMS mass spectra (in the range 100 - 200 amu) of the nebulized solutions sampled from experiment B after 50 and 150 min of reaction in the aqueous phase. The AMS-mass fraction is the signal intensity contribution of each fragment to the total signal.

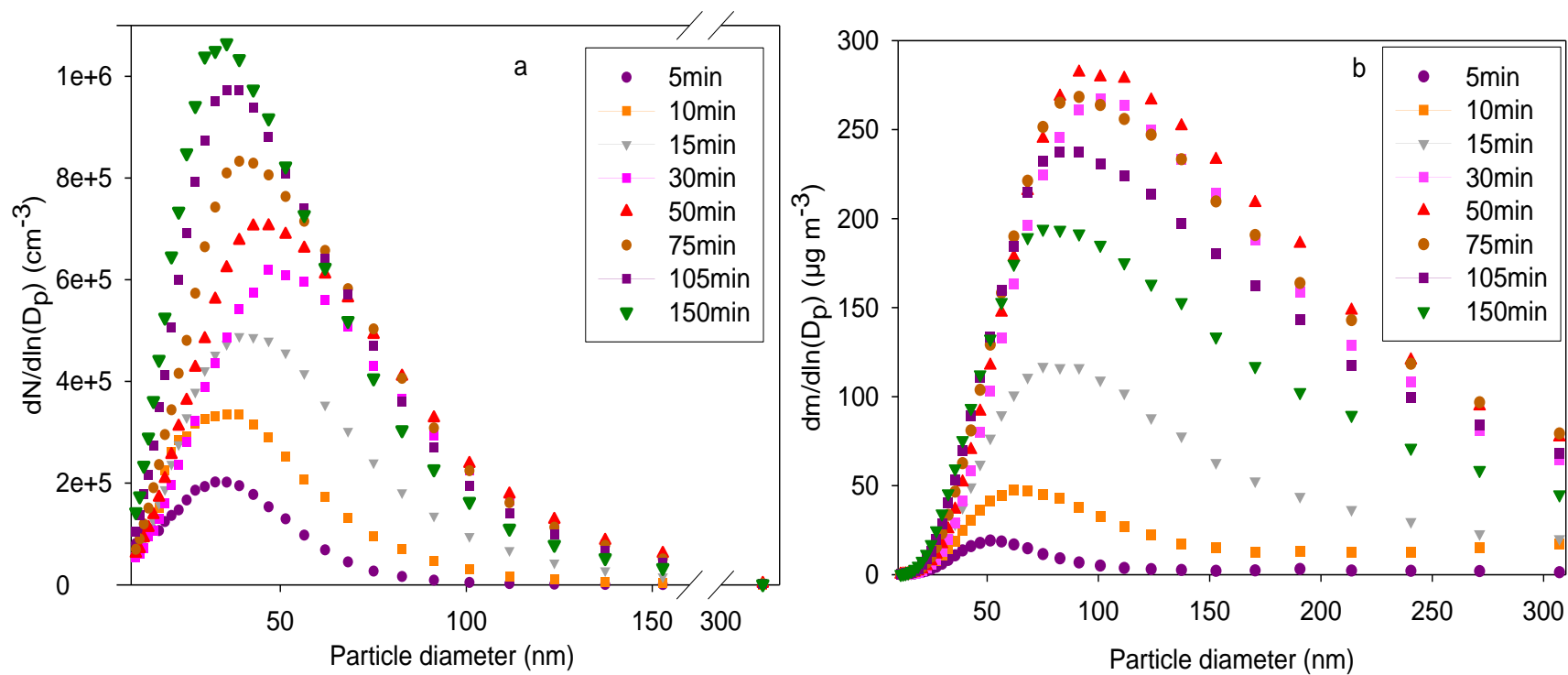


Figure 5: Evolution of particle number (a) and mass (b) size distributions for nebulized solutions sampled at different reaction times for experiment B, measured by means of SMPS. The standard deviations are smaller than the width of the symbols

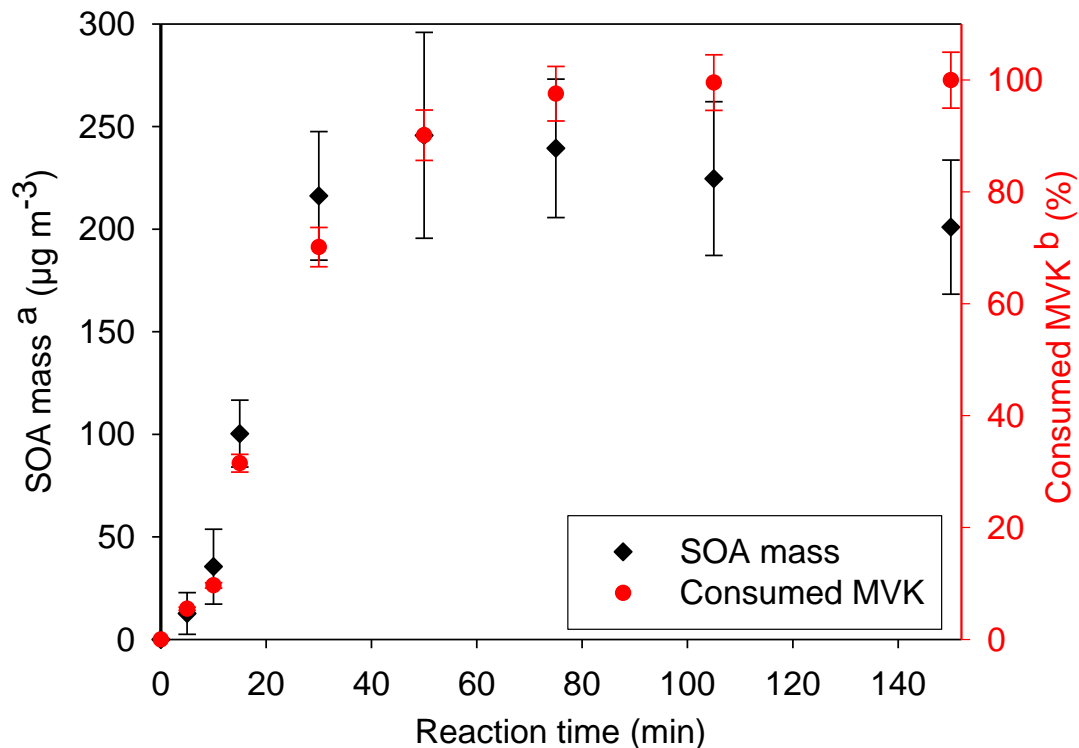


Figure 6: Time profiles of the total aerosol mass (black diamonds) from the nebulized solutions, and consumed MVK in the aqueous phase (red circles) for experiment B. ^a Values represent averages of three consecutive SMPS-measurements for each reaction time considering the corresponding density (Table 1). Error bars represent the sum of the standard deviation of these averages and the uncertainties of the density calculation. ^b % in concentration of MVK. These concentrations were determined by means of UHPLC-UV, with an uncertainty of ± 2 %;

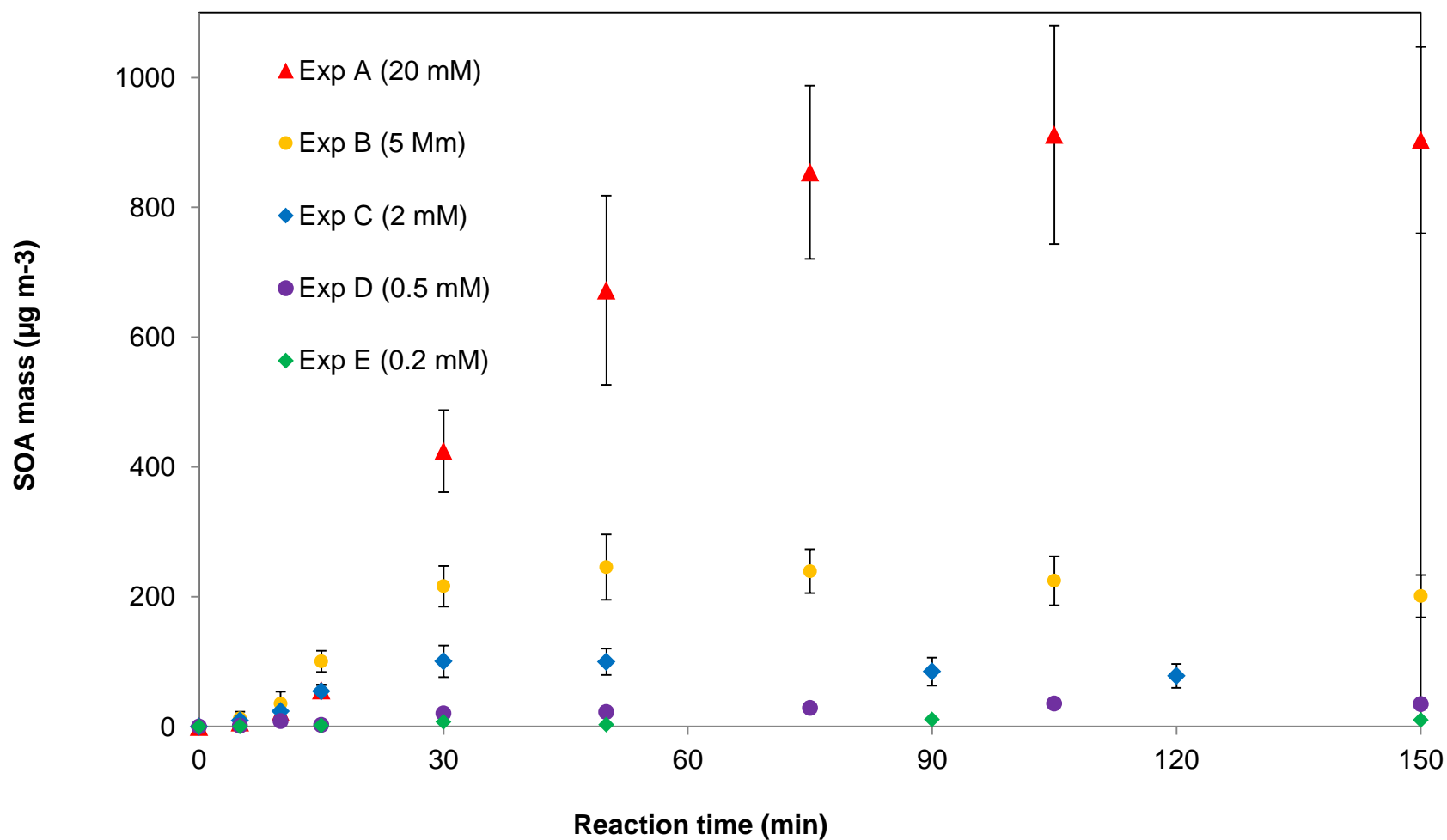


Figure 7: Influence of the initial MVK concentration on the evolution of the total SOA mass obtained from the nebulized solutions. Values represent averages of three consecutive SMPS-measurements for each reaction time considering the corresponding density (Table 3). Error bars represent the sum of the standard deviation of these averages and the uncertainties of the density calculation. For the lowest initial concentrations (experiments D and E), blank signals were subtracted, and a density of 1.1 g cm^{-3} was assumed.

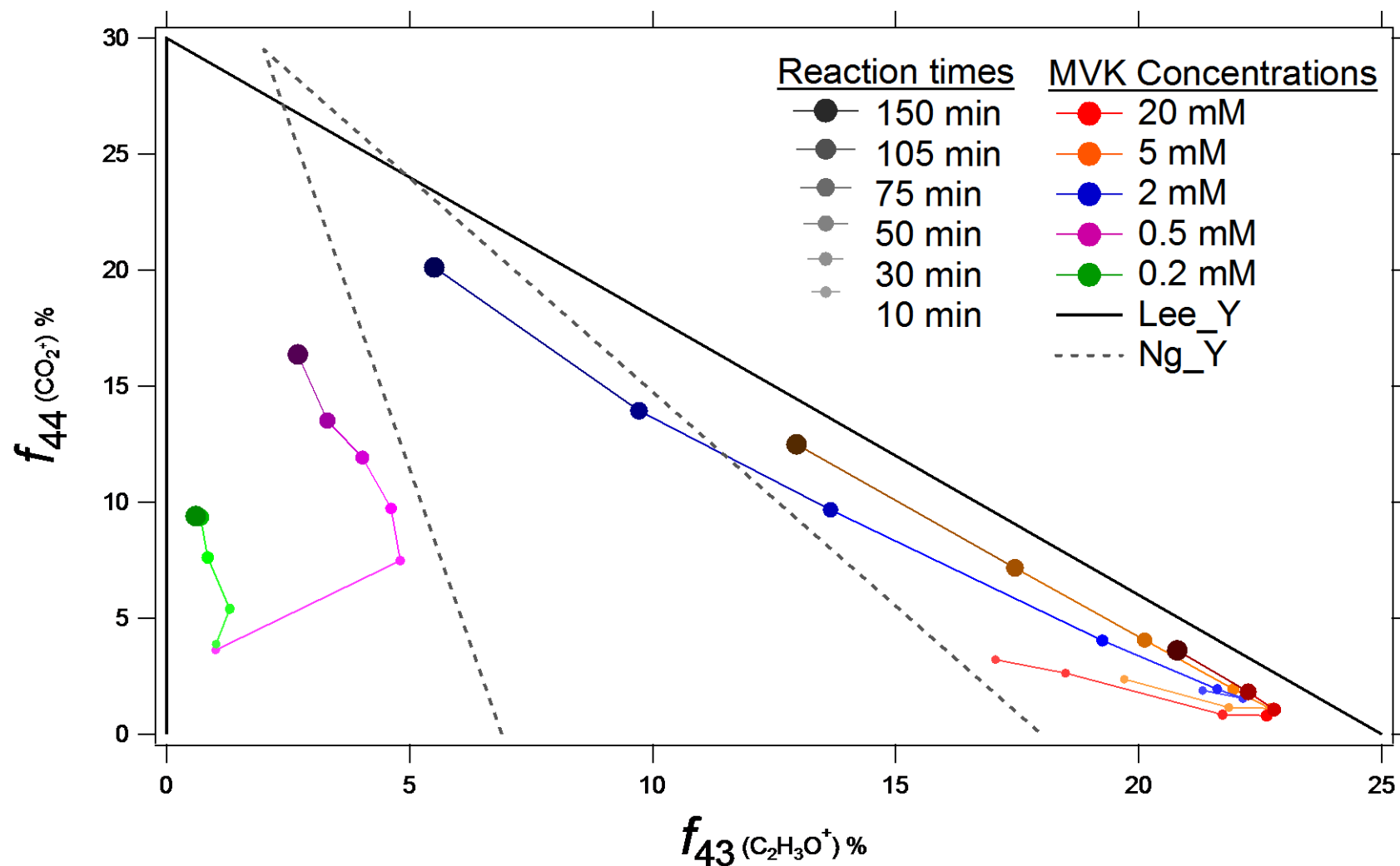
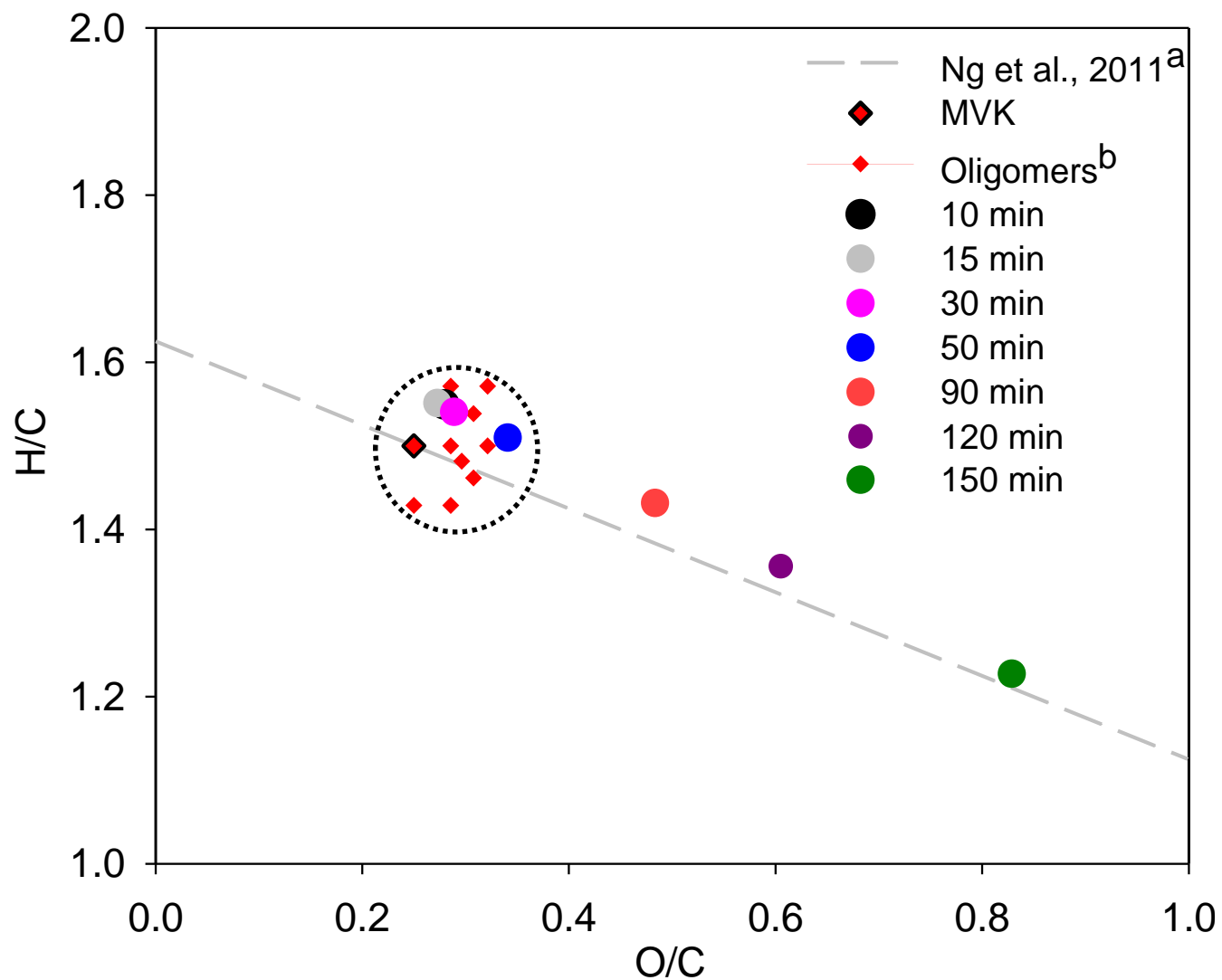
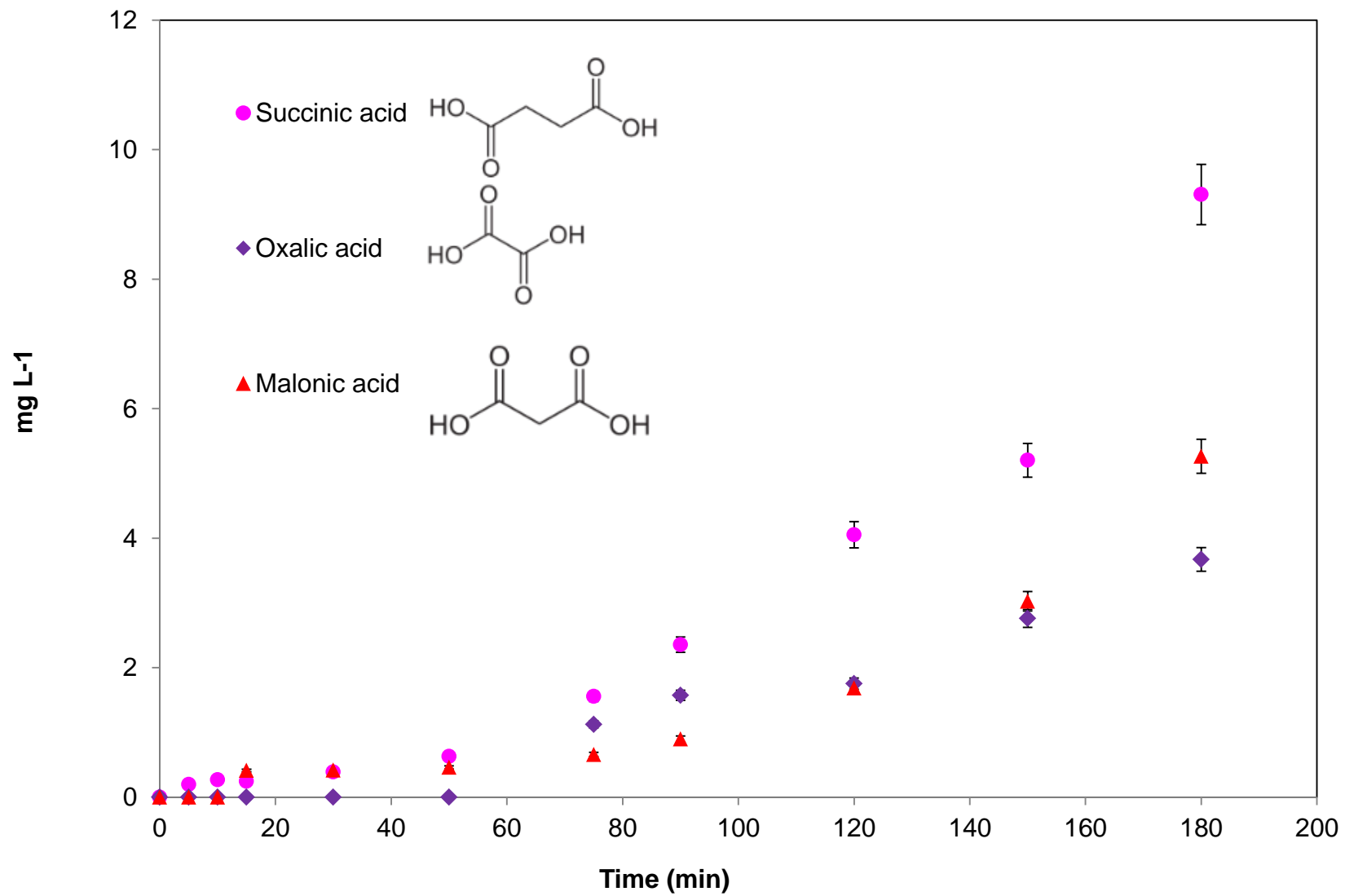


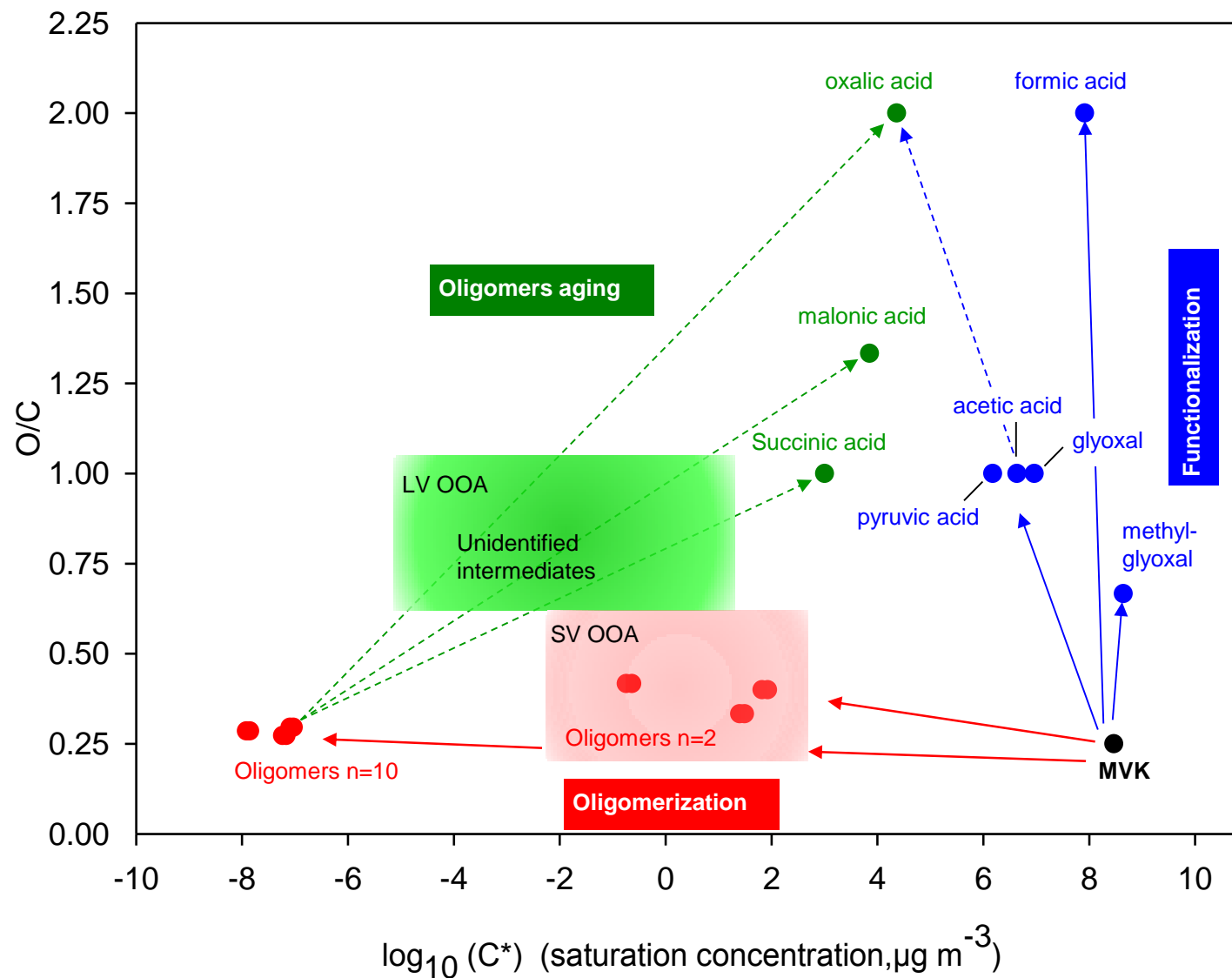
Figure 8: Fractions f_{44} versus f_{43} for the nebulized solutions from experiments A, B, C, D and E, as measured by the HR-ToF-AMS are compared to ambient air LV-OOA and SV-OOA from the compilation by Ng et al. (2010) (dashed black triangle), and are also compared to the nebulization data by Lee et al. (2011a) (dotted grey triangle). For our experiments, the signal from blank experiments was subtracted. The data are shown for experiments A, B, and C from 10 to 150 min of reaction, and for experiments D and E from 15 to 150 min of reaction. The gas/particle partitioning in our set up may alter the relative oxygenation of the OA produced, especially at low initial concentrations.



44 **Figure 9:** Van Krevelen diagram for the nebulized solutions of experiment C, as measured by the AMS. Only experiment C is shown for clarity as the data for experiments A and B are stacked together with the data shown. ^a Red diamonds represent the elemental ratios of oligomers with a Degree of Polymerization = 5 for the ten most abundant oligomer series identified by Renard et al. (2013). The black dotted circle highlights compounds with similar structures. ^b Ng et al., 2011, for details see text section 4.2.



45 **Figure 10** : Time profiles of the quantified diacids in the solutions as measured by IC-ESI-MS for experiment B ($[MVK]_0 = 5$ mM).



46 **Figure 11:** Potential atmospheric fate of MVK in the aqueous phase. X-Axis denotes volatility (\log_{10} of C^* at 298K), y-axis denotes oxidation state, approximated by O/C (Jimenez et al., 2009).